Shallow urban aquifers under hyper-recharge equatorial conditions and strong anthropogenic constrains. Implications in terms of groundwater resources potential and integrated water resources management strategies

B. Nlend, Hélène Celle-Jeanton, F. Huneau, E. Garel, S. Ngo Boum-Nkot, J. Etame

▶ **To cite this version:**

B. Nlend, Hélène Celle-Jeanton, F. Huneau, E. Garel, S. Ngo Boum-Nkot, et al.. Shallow urban aquifers under hyper-recharge equatorial conditions and strong anthropogenic constrains. Implications in terms of groundwater resources potential and integrated water resources management strategies. Science of the Total Environment, 2021, 757, pp.143887. ⟨10.1016/j.scitotenv.2020.143887⟩. ⟨hal-03236328⟩

HAL Id: hal-03236328

https://hal.science/hal-03236328v1

Submitted on 15 Dec 2022

HAL is a multi-disciplinary open access archive for the deposit and dissemination of scientific research documents, whether they are published or not. The documents may come from teaching and research institutions in France or abroad, or from public or private research centers.

L'archive ouverte pluridisciplinaire **HAL**, est destinée au dépôt et à la diffusion de documents scientifiques de niveau recherche, publiés ou non, émanant des établissements d'enseignement et de recherche français ou étrangers, des laboratoires publics ou privés.

Distributed under a Creative Commons CC BY-NC 4.0 - Attribution - Non-commercial use - International License

Version of Record: https://www.sciencedirect.com/science/article/pii/S0048969720374180
Manuscript_534036bba3bde6900c2a0d28bb1aea38

Shallow urban aquifers under hyper-recharge equatorial conditions and strong anthropogenic constrains. Implications in terms of groundwater resources potential and integrated water resources management strategies.

B. Nlend [a.d.e*], H. Celle-Jeanton [a], F. Huneau [b.c], E. Garel [b.c], S. Ngo Boum-Nkot [d], J. Etame [d]

[a] Université de Bourgogne Franche-Comté, CNRS, UMR 6249 Chrono-Environnement, 16 route de Gray, F-25030 Besançon cedex, France

[b] Université de Corse Pascal Paoli, Département d'Hydrogéologie, Campus Grimaldi. BP 52, F-20250 Corte, France

[c] CNRS, UMR 6134 SPE, BP 52, F-20250 Corte, France

[d] University of Douala, Faculty of Sciences, P.O BOX 24157, Douala, Cameroon

[e] Cameroonian Institute for Geological and Mining Research., Hydrological Research Center, P.O BOX 4110, Yaoundé, Cameroon

*Corresponding author:

Bertil NLEND

Université de Bourgogne Franche-Comté.

CNRS. UMR 6249 Chrono-Environnement.

16 route de Gray, F-25030 Besançon cedex, France

Tel: 03381666242 (from abroad: +33381666242)

Email: nlendbertil@yahoo.fr

ORCID identifier: https://orcid.org/0000-0001-7961-1901

© 2020 published by Elsevier. This manuscript is made available under the CC BY NC user license
https://creativecommons.org/licenses/by-nc/4.0/

Abstract

Humid equatorial regions are recognized as the least documented in term of hydrogeological functioning of aquifers despite the fact that they house a lot of developing countries and that groundwater is often the main water resource. Regarding this aspect, a study was conducted in sub-Saharan Africa, focusing on the Mio-Pliocene aquifer in Douala megacity (Cameroon) which is the rainiest city in West-Africa (about 4000 mm/year) with one of the greatest demographic growth rate of the African continent. Firstly, groundwater recharge rate has been calculated through water balance and Water Table Fluctuation methods. Results show that the aquifer is characterized by a high recharge of 600-760 mm/year. Then infiltration process and groundwater flow conditions have been examined by combining hydrogeological and isotopic methods. Rainwater infiltrated is recycled in the vadose zone through plants roots transpiration and groundwater flows with a Darcy velocity of 5 m/day. From the recharge area to the estuary, the mineralization increases controlled by anthropogenic activities and water-rocks interactions which are amplified by the residence time and accelerated by the hot and humid climate of Douala. The paper ends with the determination of natural background levels (NBLs) and threshold values (TV) of chemical components in groundwater to assess the contamination for different flow paths. This multi-proxy study and the establishment of NBLs and TV can be beneficial to improve groundwater resources management. Moreover, the conceptual model provided in this study could be used as a reference for porous aquifers submitted to high rainfall amount.

Keywords: urban hydrogeology; groundwater recharge, stable isotopes; geochemistry, integrated water resources management; threshold values.

1. Introduction

While many works have been published on recharge, functioning and management of aquifers in arid or semi-arid areas (e.g., Sami 1992; Allison et al. 1994, Scanlon et al. 2006, Rahmani et al. 2017), there is still very little knowledge about groundwater functioning in humid tropical regions and papers on humid tropics hydrogeology remain rare; mainly focusing on water quality and on the economic and environmental significance of this resource (Foster 1993; Foster et al. 2018; Nlend et al. 2018). Fosberg et al. (1961) physically identify these regions by: (*i*) a monthly temperature equaling or exceeding 20°C for at least eight months of the year; (*ii*) a vapor pressure and a relative humidity average of ~20 millibars and 65% respectively, for at least 6 months of the year; (*iii*) an annual rainfall exceeding 1500 mm and; (*iv*) the rain falling all year with at least six months having precipitation ≥75mm/month. They represent approximately 22% of the earth's surface (UNESCO 1990, 2000; State of the tropics 2014) and house a lot of developing countries which present the highest demographic growth rates and whose population is expected to represent 50% of humanity by 2050 (State of the tropics 2014). Wohl et al. (2012) reported then that humid tropics are dynamic environments where freshwater is under pressure from population growth, land use and climate change. In addition to their importance for the water supply, these hydro-systems are a key factor in the preservation of humid tropical ecosystems (animal-plant-soil-water), because of the intimate relationship between surface and groundwater and the frequently shallow groundwater table with abundant humid equatorial vegetation in such environments (Foster & Chilton 1993). Regarding all these aspects, there is an urgent need to increase the knowledge in aquifers functioning in humid tropical regions and peculiarly in sub-Saharan African areas which represent 30% of the humid tropics (45% in latin America and 25% in Asia) -according to State of the tropics (2014) -; and is often regarded as the world's fastest urbanizing region (Saghir & Santoro 2018).

In this objective, the Douala megacity (Cameroon, Western Central Africa) is a perfect example of a tropical area with approximately 4000 mm/yr, 230 rainy days/yr, a mean air temperature of 27°C (Tchiadeu & Olinga 2012) and a rapid urbanization process due to a demographic boom that has begun in the early 80's (Nlend et al. 2018). Douala is the economic capital of Cameroon and the most dynamic town in the Central Africa region by ensuring, for example, the transit of goods from the rest of the world to landlocked countries like the Central African Republic and Chad). The demographic dynamism of Douala is expressed by a large movement of people from the countryside to the coastal cities due to economic reasons. Indeed, this metropolis, the largest city in Cameroon with a big harbour, is highly developed with varied industries (textiles, agro-food, chemicals, glassworks, cement, wood, fertilizers, etc.). In this large city, 49% of the drinking water is produced from sub-surface by the Cameroon Water utilities (Camwater) and the Mio-Pliocene (MP) sands aquifer represents the most exploited resource. This latter is tapped both formally by Camwater and informally by many industries and people for domestic uses and drinking water supply purposes (Mafany 1999). However, the anthropogenic fingerprint at Douala has already showed harmful effects on local water resources as it experienced cholera epidemics in 2004 (Guevart et al. 2006) and 2012 (Ketchemen-Tandia & Banton 2012), making access to clean water a major priority for populations.

Regarding these important issues, this article follows the previous studies which have mainly dwell long on groundwater quality (Takem et al. 2010; Kopa et al. 2012; Ngo Boum et al. 2015; Fantong et al. 2016; Tatou et al. 2017; Ketchemen-Tandia et al. 2017 and Wirmvem et al. 2017) but the hydrogeological functioning of the MP aquifer is still very little known. Therefore, this research is a first attempt to conceptualize the functioning (recharge, infiltration, groundwater flow organization and acquisition of mineralization) of the main groundwater resource of the city which is the MP aquifer in a context of high rainfall regime

100 by using an innovating combination of hydrogeological, isotopic and chemical methods
101 coming both from historical data collection and new investigations over the study area. Beside
102 the hydrogeological and water quality analysis, the paper aims at determining the natural
103 background levels (NBLs) and proposes threshold values (TVs) of groundwater chemical
104 components of the region in order to propose management tools able to provide guidance for
105 the future exploitation of groundwater resources. Such type of investigation can be used as a
106 reference for urban porous aquifers in humid tropical areas and in the establishment of
107 improved integrated water management strategies in Africa.
108

109 ## 2. Framework of the study region

110 ### 2.1. Location and topography

111 The Douala region (03°45'N – 04°20'N, 09°34'E – 10°00'E) is a coastal site (~ 33 km to the
112 ocean) located approximately 70 km southwest to the Cameroon Mount (~ 4100 masl),
113 covering an area of more than 300 km² on the Gulf of Guinea, in the Republic of Cameroon
114 (Fig. 1).

115 Figure 1
116

117 The relief is little contrasted with altitudes varying between ~3 masl on the estuary zone to
118 about 70 masl in the eastern side of the region (Figure 2).

119 Figure 2

120 ### 2.2. Climate

121 The climate of Douala is characterized by strong marine influences (Olivry 1986). The annual
122 rainfall regime is unimodal with a long rainy season from March to November and a very

123 short “dry season” in December–February (Fig. 3). Considering the 65 years (1951-2016) of
124 rainfall recorded at Douala meteorological station (04°01’N, 09°42’E), the annual average is
125 3854.3 mm, the maximum and minimum monthly values are respectively measured in August
126 (742.4 mm) and December (34 mm). These very rainy conditions throughout the year make
127 Douala to be considered as a singular hyper-rainy city.

128 Figure 3

129 The peculiar climate of Douala is also linked to the relative uniformity of air temperature and
130 very high atmospheric humidity conditions. The mean annual temperature is 27°C; lowest and
131 highest temperatures are observed respectively in August (25.4 °C) and February (28.6 °C),
132 giving low annual thermal amplitude of 3.2 °C (Fig. 3). The relative humidity (records of
133 1971-2009) ranges between 79% and 90% during the rainy season (March to November) and
134 between 77% and 81% during the dry season (December to February), with an annual mean
135 of 85%.

136 **2.3. Hydrography**

137 The wet conditions described above are reflected at the surface by a very dense hydrographic
138 network (Fig. 2) confirming the observations of Braune & Xu (2009) in this part of Africa.
139 Apart from the swamps that cover lowland areas, two main watercourses drain the study area:
140 the Wouri and the Dibamba Rivers which present many tributaries (Fig. 1 & 2). Both the
141 Wouri and the Dibamba dendritic drainage basins discharge into the Atlantic Ocean where
142 tides entering the estuaries make them vulnerable to seawater intrusion (Onguene et al. 2015).
143 The hydrological regime of these rivers is similar to that of rainfall. Low flow are registered
144 from November to December (discharge <200 m^3/s) and then increase slowly up to June and
145 abruptly up to September when it reaches a maximum value of 900 m^3/s (Olivry 1986). At

146 this moment, the soil often becomes saturated and the streams overflow their channels causing
147 floods favoured by the low altitude of the area. Then, from October discharge is decreasing.

148 **2.4. Soils and vegetation**

149 Douala has two types of soils: ferralitic and hydromorphic (Segalen 1967; Zogning 1987;
150 Ndome 2010). In both cases, the authors identified a large proportion of fine and coarse sands
151 (45 to 80%), and clays (10 to 50%). The proportions of kaolinite (50-60%) are the most
152 important while goethite (35-42%) is significant and gibbsite (2-10%) is negligible
153 (Ngeutchoua 1996). Ferralitic and hydromorphic soils occupy respectively 80% and 20% of
154 the study region. The latter is mainly observed in alluvial plains and valley bottoms.

155 The vegetation is that of low altitude rainforest with large mangroves along the coast,
156 evergreen forest and some plantations (banana, corn, sugar cane, fruits, etc). Riparian
157 vegetation is observed near the valleys and depression areas (Din Ndongo 2001).

158

159 **2.5. Geology and hydrogeology: emphasis on Mio-Pliocene formations**

160 The Douala region is constructed on a 5 km-thick sequence of unconsolidated to semi-
161 consolidated sedimentary rocks going from Pleistocene to Aptian (Fig. 4; Regnoult 1986).
162 These sediments are associated to tectono-sedimentary dynamics which prevailed during the
163 opening of the South Atlantic and the formation of West African passive margin (Moulin
164 2003; Helm 2009). Continental in the eastern part of the basin, sediments progressively move
165 westward to marginal sea, continental shelf and deep seabed environments. They can be
166 divided into seven formations from the bottom to the top (Fig. 4): *i*) Mundeck's
167 conglomerates and sandstones (Apto-Albian), *ii*) Logbadjeck's conglomerates, sandstones and
168 limestones (Turonian-Santonian), *iii*) Logbaba's sands, sandstones and clays (Campanian-
169 Maastrichtian), *iv*) Nkapa's limestone, sandstone, marl and shales (Paleocene-Eocene), *v*)

Souellaba's clays and sands (Oligocene-Lower Miocene), *vi*) Matanda's clays, sands and gravels (Upper Miocene-Pliocene) and *vii*) Wouri layers (Quaternary) consisting of clays, sands and gravels (Dumort 1968; Njike Ngaha 1984; Regnoult 1986; Nguene et al. 1992; SNH/UD 2005; Manga 2008; Njoh et al. 2014; Njoh & Petters 2014; Njike Ngaha et al. 2014).

Figure 4

The Mio-Pliocene aquifer is represented by Souellaba and Matanda formations, overlying the Eo-Oligocene and covered in some places by the Quaternary sediments 20 to 70 m thick (Feumba 2015). It consists in a multi-layered aquifer separated from more superficial and deeper aquifers by discontinuous clay layers. Its thickness globally increases NE to SW (Fig. 4). Although many lithological lateral variations, the global structure of the MP aquifer from the top to the bottom can be described as follows (Table 1) by using well logs and previous works on hydrogeology (Bourgeois 1977 and Ketchemen-Tandia 2011):

(i) the Pliocene is clayey, clayey-sandy and sandy-clayey. Its depth generally does not exceed 40 m;

(ii) the Upper Miocene consisting of coarse grained sands with gravel intercalations. Sandy sequences, slightly silty and calcareous, appear well developed at the NW of Douala where their thickness exceeds 200 m (Bourgeois 1977);

(iii) the Lower Miocene formation made up of cross-bedded sands and marked by some passages of lignite and limestone.

Table 1

196

197 Separated by a clay layer, the difference between Mio-Pliocene and Quaternary formations
198 lies in the lithology; Quaternary sands are finer than those of the Mio-Pliocene.
199 The lateral variations observed in lithology of the MP aquifer are also reflected in
200 hydrodynamic settings (Table 2). High values of standard deviation (Table 2) in
201 transmissivity and hydraulic conductivity suggest an important anisotropy of the MP aquifer.

202

203 Table 2

204 **3. Methods of investigation**

205 **3.1. Inventory of sampling points**

206 Wells logs and results from hydraulic testing, when available, have been compiled from
207 previous projects in the study area. Indeed, priority has been given to wells having this basic
208 information and which are still used currently by local populations. In addition to this
209 inventory, a field campaign was conducted to target springs in the study area. Finally, a total
210 of 58 sampling points, including 43 wells (26 boreholes and 17 hand-dug wells) and 15
211 springs on the MP formation have been selected according to their distribution over the
212 Douala region. In general, hand-dug wells tap water at shallow levels (<18 m) while
213 boreholes will correspond to water from more important depth (maximum = 90 m). Boreholes
214 are often equipped with foot or hand pumps or directly connected to a faucet. The only
215 disadvantage of this engineering structure in Douala is that they are most of the time screened
216 at several depths. For some wells, this can complicate the understanding of groundwater flow
217 and hydrochemical processes that take place within the different levels. Springs encountered
218 in the study area are located at the bottom of steep slopes, bordering important marshy areas.

219

220

221 **3.2. Field measurements, sampling and analytical procedures**

222 Groundwater sampling and *in situ* measurements (water levels and physicochemical
223 parameters) were achieved in February 2017. Springs have been sampled directly at their
224 outflows. Wells and boreholes have been sampled by pumping, using the in-situ equipment.
225 Assuming the fact that wells in Douala are daily used for domestic supply, it was considered
226 during the campaign that there is no stagnant water within wells and that their purge is already
227 achieved. The depth of groundwater in the well relative to the soil surface *i.e* water table (h)
228 was measured by using a potentiometric probe. Knowing the altitude (Z) of the sampling
229 point, the water table was converted in potentiometric level (H) through the formula H = Z –h
230 and by considering the height of the well edge. Physicochemical parameters (pH, electrical
231 conductivity, water temperature and dissolved oxygen) were measured using a WTW
232 2FD46G multi-parameter. Measurements have been validated only after all of the in situ
233 parameters reached the stability criteria (Rey et al. 2017) for three consecutive measurements
234 separated by 5-minutes intervals. Alkalinity measurements were performed using a digital
235 titrator (HACH). Samples for major ions analysis (Cl^-, NO_3^-, SO_4^{2-}, HCO_3^-, Na^+, K^+, Mg^{2+} and
236 Ca^{2+}) were collected in two 30 mL polyethylene bottles after filtration through 0.45 µm
237 nitrocellulose membranes. Samples for cations analysis were acidified with ultrapure HNO_3^-
238 at 70%. Bottles were filled to the top with no headspace and kept at 4°C until analyses.
239 Chemical analyses were conducted at the Hydrogeology Department of the University of
240 Corsica, France by ionic chromatography using a Dionex ICS 1100 chromatograph. The
241 quality of the analysis was checked by calculating the ionic balance error: analyses were
242 rejected if the ionic balance error was greater than 5%.

243 Samples for stable isotopes of the water molecule were stored in 20 mL amber glasses bottles.
244 All care was taken to avoid evaporation by taking water directly in the well. As for chemistry,

bottles were filled to the top with no headspace and samples were kept cool until being transferred to the laboratory where measurements were performed at the Hydrogeology Department of the University of Corsica, France using a liquid–water stable isotope analyzer DLT-100 (Los Gatos Research) according to the analytical scheme recommended by the IAEA (Penna et al. 2010). Values are reported in per mil units (‰) compared to Vienna Standard Mean Ocean Water standard (VSMOW). The quality of the isotopic analysis was checked using a standard deviation up to 1‰ for δ^2H and up to 0.1‰ for $\delta^{18}O$.

4. Results and discussion

4.1. Estimation of Mio-Pliocene aquifer recharge

In this paper, two methods were applied: a water balance and a physical method on saturated zone (Water Table Fluctuations, WTF). These approaches were chosen given the availability of required data. The choice of these methods was driven by the goal to obtain an average rate of recharge for the aquifer. Moreover, WTF and water balance methods are known to be well applied both in humid and semi-arid contexts requiring low data and at relative low costs (Scanlon et al. 2002). The first one relying on groundwater data and the second one on climate data.

Water balance calculation

Recharge is usually calculated as the remainder when losses identified in the form of runoff and evaporation, have been deducted from precipitation (see equations 1 and 2). The term "evaporation" here envelops transpiration.

$$P = R + Ea + \Delta SWS + Ieff \quad (1)$$

$$Ieff = P - (R + Ea + \Delta SWS) \quad (2)$$

P is the monthly rainfall, Ea the real evapotranspiration, R the surface and sub-surface drainage, and ΔSWS the storage variation in the unsaturated zone. The rainfall used in the balance is given by the measurements at the Douala meteorological station. Real evapotranspiration (Ea), described in detail by Allen et al (1991), was estimated from the corrected potential evapotranspiration (PETcor) and average Kc values per crop (Allen et al. 1998). PETcor was estimated by correction of the potential evapotranspiration calculated by Thornthwaite's equation, as proposed by Medeiros et al. (2012). All these annual average parameters can be considered as homogeneous spatially regarding the topography of the study area.

Therefore, taking into account the potential evapotranspiration, actual evapotranspiration and rainfall amount recorded month by month the yearlong at Douala; the Figure 5 shows that the MP aquifer is potentially recharged from June to November when P > PET and when the soil water deficit is filled. From December to February, P<PET and PET > Ea, then the recharge of soil reserve is null and the groundwater table is down. Indeed, the potential recharge follows the rainfall regime.

Figure 5

This potential recharge of 2556.5 mm corresponds to effective infiltration plus runoff. However, for the study area, no experimentally measured surface drainage data were available for the analyzed period. The data used in this paper are from Emvoutou (2018) who used remote sensing and GIS approach by considering: land use/land cover, drainage density, topography and slopes for the 2000-2004 period. The average value obtained is estimated at 46.4% of annual rainfall amount. Thus, the infiltration can be estimated at 767 mm/year i.e approximately 20 % of rainfall amount.

293 *WTF approach*

294 Based on the premise that rises in groundwater levels in shallow aquifers are due to recharge
295 water arriving at the water table and going immediately into storage (Healy & Cook 2002),
296 the water table fluctuation method can be applied here for estimating groundwater recharge.
297 The recharge rate can be obtained by applying the following equation:

298 $$\mathrm{Ieff} = \mathrm{Sy}\ \frac{\Delta h}{\Delta t} \qquad (3)$$

299 Eq. (3) assumes that water that reaches the saturated zone is immediately stored and the other
300 components of the subsoil water balance (underground evapotranspiration, base flow, inflow
301 and outflow) are zero during the period of recharge.
302 "Sy" is the specific yield, approximately equal to the storage coefficient. It is the volume of
303 water released from a unit volume of saturated aquifer material (Maréchal et al. 2006). "h" is
304 the water table height and "t" is time.
305 In this paper, empirical value of Sy provided by Johnson (1967) has been used, while values
306 of "h" come from the monthly monitoring carried out by Feumba et al (2011) in Douala. They
307 reported that the lowest depth to water (2 m) is observed in August while the highest one is in
308 December (9.8 m). Therefore, the fluctuation of water table is ranging between 2.00 and 9.80
309 m thus giving $\Delta h = 7.8$ m.
310 By considering the nature of soils (and the upper levels of MP) mainly made of sandy clay
311 materials, and if it supposed that the studied aquifer material is homogenous vertically and
312 laterally, the specific yield of 7% defined by Johnson (1967) can be used here to determine
313 the aquifer recharge according to the equation 3.
314 By applying the formula presented in equation 3, recharge is then calculated from January
315 2010 to December 2010 thanks to the monitoring carried out by Feumba et al (2011). An
316 average value of 546 mm has been obtained. Since the annual rainfall amount recorded in
317 2010 is 3585.2 mm, the recharge coefficient (I_{eff}/P) is approximately equal to 15%.

318 The small gap between the two calculated values from water balance and WTF can be
319 explained by:
320 (*i*) the evaluation of water level at the period of one year which is not sufficient. (*ii*) the
321 application of WTF method at a monthly scale can underestimate the recharge. For instance,
322 if there is a small amount of recharge that is less than drainage from the water table, then the
323 water table will continue to drop but at a slower rate.
324 In summary, we observe that the aquifer recharge period corresponds to six successive
325 months. By taking into account the replenishment of soils reserves, we can conclude that the
326 aquifer is recharged approximately all the yearlong. This indicates that the studied aquifer
327 presents excellent quantitative potential, especially for water supply. The recharge rate of
328 15% - 20% (578.2 – 732.3 mm/year) of annual rainfall amount is lower than that highlighted
329 by model analysis (Mohan et al 2018) -where the annual recharge rate is estimated at more
330 than 1 m-, but similar to that obtained in other similar humid tropical areas such in Ghana and
331 Benin where there is also ferralitic soils (Obuobie et al. 2012; Kotchoni et al. 2019). In the
332 next section we will identify the recharge areas and discuss about the infiltration process and
333 groundwater flow within the aquifer.
334 **4.2. Location of recharge areas, infiltration process and analysis of groundwater flow**
335 *Location of recharge areas*
336 The potentiometric map of the MP aquifer is presented on Fig. 6. We identify on this map,
337 two piezometric domes in Ndogpassi – Nyalla (SE) and Kotto (NE) corresponding to most
338 elevated points (66 and 50 m.a.s.l respectively) which can be considered as focused recharge
339 areas of the MP aquifer at Douala. Indeed, the piezometric structure of the aquifer is in good
340 agreement with the topography (Fig. 2) of the region as described in section 3.1. This feature
341 is a characteristic of unconfined aquifer.
342

343 Figure 6

344 *Infiltration process*

345 Water stable isotopes (Fig. 7) show that rainwater infiltrates the soil without undergoing
346 evaporation phenomenon. Following Barnes & Allison (1988) and Lu et al (2017)
347 observations in wet soils, the zone in which significant evaporation occurs is narrow or
348 inexistent. This is in agreement with the hyper-humidity conditions characterizing the study
349 region. However, MP groundwater are ranging from -5.1‰ to -3.1‰ $\delta^{18}O$ and -25.7‰ to -
350 9‰ $\delta^{2}H$ with mean values of -3.5 $\delta^{18}O$ and -13 $\delta^{2}H$ while the weighted mean value of rainfall
351 corresponds to -2.8‰ $\delta^{18}O$ and -12.2‰ $\delta^{2}H$. This is particularity well displayed on Fig. 6
352 where groundwaters plot above the Douala and Global MWL (Meteoric Water Line). Such
353 result suggests a complexity in infiltration mechanisms.

354

355 Figure 7

356

357 This difference between isotopic composition of rainwater and groundwater at Douala, can be
358 further examined through the analyses of the deuterium excess ("d-excess"; Eq. (4);
359 Dansgaard 1964).

360 $d = \delta^{2}H - 8\delta^{18}O$ (4)

361 The d-excess weighted mean in Douala precipitation (2006–2018) is 10.4 ‰, close to d-
362 excess of the GMWL (d-excess = 10‰; Fig. 7 & 8) thus reflecting an oceanic origin of the
363 water vapor (Craig 1961). In aquifer, $d\text{-excess}_{mean}$ = 14.8‰. Approximatively, the same value
364 is observed both in shallower and deep water. D-excess value of MP groundwater is
365 significantly higher than the one recorded in the recharge water (Fig. 8). However, it is similar
366 to that recorded in rainfall at Bangui (13.5‰) and Kisangani (15‰; IAEA/WMO 2019) in the
367 Congo basin (Fig. 8) where there is an influence of continental recycling (Ketchemen et al.

2011; Risi et al. 2013; Nlend et al. 2020). Could this process occur within the vadose zone through the transpiration of plants roots? According to Blavoux (1978) and Barnes & Allison (1988), transpiration both removes some enriched water and causes a water flux at depth which is greater than the evaporative flux at the soil surface. Indeed plants transpiration favors root water transport from deeper to shallower soil layers, leading to isotopic depletion (Lu et al. 2017). Therefore, the d-excess-shift observed between recharge water and groundwater in Douala can be attributed to plants transpiration within the unsaturated zone. Soil water use by plants can be dominant when the soil water reserves are null (December-February) and even during the replenishment from March to May (Fig. 5). Barbeta and Peñuelas (2017) reported that this plant groundwater uptake represents on average 49 % of transpired water in dry seasons and 28 % in wet seasons worldwide. This hypothesis is supported by the common occurrence of deep roots which can exceed respectively 3.5 m and 1 m for woody and herbaceous species of the study region. In addition, according to Barbeta and Peñuelas (2017), as Douala is a flat area with landscape mostly represented by plain and riparian zones, the contribution of groundwater to transpiration must be particularly significant. The absence of significant difference between isotopic compositions of shallower and deep water (respectively hand dug-wells and boreholes, Fig. 7) may illustrate the influence of transpiration on shallow groundwater stable isotopes. The changes from rainwater to aquifer are likely a result of the lateral roots extracting water from the subsoil and redistribution to the superficial layer, The same observation was done by Lu et al (2017) thanks to experimentation employing customized transparent chambers coupled with a laser-based isotope analyzer measuring continuously near surface variations in the stable isotopic composition of evaporation (E, δ_E), transpiration (T, δ_T) and ET (δ_{ET}) to partition the total water flux.

392 Fig.7 shows also the existence of paleo-groundwater within the MP multilayer aquifer system.
393 Indeed the sample of Yabea exhibits a strongly depleted signature (-5.1‰ $\delta^{18}O$) compared to
394 the other points. It is a borehole of 95 m deep with a water table at 54 m. According to
395 Ketchemen-Tandia (2011) this groundwater resource from the most confined part of the
396 aquifer, exhibiting depleted isotope values, has zero tritium content; while tritium contents
397 recorded in springs and hand-dug wells vary from 2.1 to 5.9 TU, in good agreement with the
398 regional rainfall input (GNIP data at the Ndjamena station; IAEA/WMO 2018). This indicates
399 that the groundwater of Yabea is, for sure, originating from a recharge having occurred prior
400 to the atmospheric bomb tests (i.e. before 1953; Fontes 1983) and therefore is more than 70
401 years old and probably corresponding to a palaeorecharge episodes dating a few millennials
402 ago considering the amplitude of the isotopic depletion (Jirakova et al., 2011) as already
403 described in the Western Africa (Huneau et al., 2011). Therefore the studied aquifer gathers
404 water from recent infiltration and paleo-recharge.
405
406 Figure 8
407
408 *Analysis of groundwater flow*
409 Water reaching the saturated zone globally moves from the eastern side of the study region
410 toward the discharge area in the Wouri estuary zone (Fig. 6).
411 However, the variable groundwater flow directions and the variability of the distance between
412 the potentiometric surface contours (Fig. 6) characterize a non-uniform flow regime.
413 Potentiometric surface contours become more and more distant from the recharge area,
414 indicating a dominance of permeable formations towards the estuary in agreement with
415 geological/hydrogeological description. Moreover, the general shape of the potentiometric
416 surface is convex, showing a radial aquifer with divergent streamlines contrary to semi-arid

417 and arid regions where convergent streamlines towards the water course axis are generally
418 observed (e.g., Ouali et al. 1999; Lienou et al. 1999).
419 Hydraulic gradients (*i*) from upstream to downstream, calculated along the transect line C-D
420 (Fig. 6) from hand-dug wells; vary between 3.5‰ and 2.1‰ with a mean of 2.3‰
421 characteristic of unconfined aquifer conditions. Thanks to this mean value of *i*, and assuming
422 a porosity (n) of 0.07 for MP sands and an average hydraulic conductivity (K) of 1.5×10^{-3}, a
423 calculation of groundwater velocity (V = k * *i*/n) has been performed. V was estimated to
424 $4.9\text{x}10^{-5}$ m/s or 5 m/day. Therefore, it would take 70 years for water to travel from the
425 upstream zone (at PK 13) to the estuary area (Fig. 6). This Darcy velocity is very important
426 compared to that generally observed in porous media (Piccinini et al. 2016). It may be
427 attributed firstly to the high hydraulic conductivity of the aquifer and secondly to the high
428 rainfall recorded at Douala which leads to shallow groundwater table and therefore contribute
429 somehow to high values of hydraulic gradient as observed.
430 In the discharge area, the MP aquifer can develop interactions with the Wouri and Dibamba
431 Rivers (Fig. 6). It can be suspected that when there are superimposed, a natural upward water
432 flux from the MP to the Quaternary aquifers should occur. Moreover, in this discharge zone,
433 groundwater can also be influenced by ocean tides. However, regarding the geographical
434 position of the aquifers (Fig. 6), Quaternary sands seem to be more vulnerable to saline
435 intrusions than the Mio-Pliocene formation. Finally, it is worthwhile noting that groundwater
436 discharge also occurs at numerous springs in the study area due to very local topographic
437 control.

438 In summary, the keys messages in this section are: (i) rainwater reaches the saturated zone
439 without undergoing evaporation; (ii) the hyper-rainy conditions contribute directly or
440 indirectly to water recycling within the vadose zone and to maintain the groundwater at a
441 shallow level even during the dry season.

In the next section we will investigate which factor controls the water chemistry along the flow and especially if there is any influence of the regional hyper-recharge rate.

4.3. Water chemistry

Main features

As shown in Table 3, groundwater temperatures (median values of 28.6°C, 28.2°C and 27.9°C respectively for boreholes, hand-dug wells and springs) are close to that of air temperatures in February (26.9°C to 30.5°C with a mean of 28.6°C) when the field measurements were carried out. It is clear that temperatures increase slightly with the depth as water from boreholes present the highest values in term of maximum, mean and median (Table 3). This can probably be associated to the geothermal gradient. The pH values show a wide range from strong acidic conditions to slightly alkaline (Table 3) thus reflecting various inputs into the aquifer system. However, when considering mean and/or median values (Table 3), the acidic character of MP water is obvious. The electrical conductivity (EC) in boreholes, hand-dug wells and springs range from 13.6 to 1632 µS/cm, 47 to 1048 µS/cm, and 111.8 to 375 µS/cm respectively (Table 3). As for pH values, this tends to reflect various influences on MP groundwater system. Nevertheless, the median EC in boreholes is significantly lower than those in hand-dug wells and springs. Therefore, the deeper the water flows, the more the groundwater mineralization decreases. It is already possible to hypothesize that the shallower aquifer system is the most affected by various inputs entering the system and peculiarly by anthropogenic factors such as: industrial effluents, water from pit latrines and leaking of solid waste.

Table 3

Dissolved oxygen (DO) concentrations show wide range of values from 2.3 mg/l to 7.8 mg/l, 2.2 mg/l to 7 mg/l and 2 mg/l to 7.8 mg/l for boreholes, hand-dug wells and springs respectively (Table 2). This heterogeneity in DO values can be related to microbial activities within the different flow paths of the Mio-Pliocene (Keesari et al. 2015). On the other hand, the fact that most boreholes are screened at different depths could affect the redox conditions within the system.

Concerning the major ions chemistry, NO_3^- is the dominant anion in boreholes and springs accounting respectively for 74% and 64% of the total major ions; after which the concentrations of anions in groundwater types follow the order $Cl^- > SO_4^{2-} > HCO_3^-$. In water from hand-dug wells there is no dominant anion; Cl^-, SO_4^{2-} and NO_3^- present approximately the same percentage (around 33%). In contrast, the concentrations in major cations are dominated for each sample by Na^+ followed by Ca^{2+}, K^+ and Mg^{2+}. This order of abundance of ions is in agreement with the hydrochemical types observed on the Piper diagram (Fig. 9) with a clear abundance of Na-K-Cl water types for the different flow paths. However, it is worthwhile noting that the borehole sample of Yabea (the most depleted in stable isotopes; Fig. 7) is the only one presenting a Ca-Mg-HCO_3 water type. This water-type reflects a lack of anthropogenic influence on this water and a predominance of geological natural processes on groundwater chemistry.

Figure 9

Evolution of major ions chemistry along a flow-path

The evolution of concentrations in major ions along the E-F transect (Fig. 6) is displayed on Figure 10. Only boreholes samples are considered on this flow-path since they appear to be

489 less influenced by human activities. It concerns the settlements of Nkolbong, Parizo,
490 Ndogpassi, KM5, Mboppi and Essengue located respectively at 16, 14, 12, 6, 4 and 2 km
491 from the sea. EC increases along the flow-path, from 32 to 1632 µS/cm. The lowest
492 concentrations characterize the recharge area (Nkolbong and Prizo, Fig. 6) while the highest is
493 observed close to the discharge area (Mboppi and Essengue).
494
495 Figure 10
496
497 Concentrations in major ions globally increase along the flow. Cl^-, HCO_3^-, Mg^{2+}, Na^+ and K^+
498 present the same behavior along the flow-path while Ca^{2+} and SO_4^{2-} also evolve in parallel,
499 decreasing abruptly close to the estuary involving specific control on groundwater chemistry
500 in the discharge area. The case of NO_3^- is more peculiar. Concentrations in this element vary
501 significantly along the flow path. Lowest values are found both in the recharge zone and near
502 the estuary. Moreover, NO_3^- in boreholes, hand-dug-wells and springs do not exhibit any
503 relationship with DO reflecting strong spatial variations of redox conditions. As many sub-
504 Saharan African metropolis, the high level concentrations in nitrates can be linked to local
505 pollution effects showing probably an input of latrine effluents (Lapworth et al. 2017).
506 Following these two previous sections describing the main features and the evolution of
507 groundwater chemistry along the flow, the next section will aim at determining the
508 hydrochemical processes involved.
509
510 *Processes controlling water chemistry*
511 Generally, the soluble ions concentrations in groundwater are partly deriving from the
512 precipitation input, evaporation, dilution, water rocks interactions, residence time and
513 anthropogenic factors. All the natural processes can be investigated through Gibbs diagram

514 which is helpful to discriminate geochemical evolutions in groundwater. A Gibbs diagram has
515 been drawn for boreholes groundwater on Fig.11. It shows that groundwater has been affected
516 largely by water-rock interaction (Figure 11) even if three groups can be separated: (*i*) the
517 group of precipitation dominance characterized by low mineralization ($13.6 < EC < 19$ and
518 $3.2 < TDS < 11.5$) suggesting a recent infiltration of rainwater in the aquifer system, (*ii*) the
519 group of water-rock reactions with samples characterized by a freshening process due to
520 important recharge conditions and (*iii*) the group of water-rocks reactions with rock
521 dominance represented only by the sample of Yabea. This sample presents a high value of
522 TDS (EC = 431 µS/cm) with low concentration in Na^+. The Gibbs diagram confirms that
523 water from this borehole may be an old groundwater in the deep part of the aquifer system.
524 Indeed, a significant time of water-rocks interactions would explain the mineralization as well
525 as lower content in Na^+ may refer to a groundwater reservoir protected from anthropogenic
526 influences.
527
528 Figure 11
529
530 In summary, it is clear that the water residence time is a control factor of groundwater
531 chemistry. In this study, the long residence time of groundwater leads to a Ca – HCO_3 water
532 type with high TDS (see Fig. 9) and no evidence of human pollution.
533
534 However, details must be provided concerning the water-rock interaction process highlighted
535 on the Gibbs diagram (Fig. 11). It is a relatively broad classification that may include many
536 kinds of processes such as silicate weathering, carbonate dissolution, and evaporate
537 dissolution. In the present case, the fact that 69% and 88% of samples have respectively a
538 molar ratio higher than 2 and 1 - respectively for Ca^{2+}/Mg^{2+} and Ca^{2+}/Na^+ ratios - indicates a

predominance of silicate weathering process in groundwater chemistry (Lee & Strickland 1988; Lakshmanan et al. 2003; Rajmohan & Elango 2004). The lithology of the strata in the study area, consisting of sands and clays and the mineralogy of the aquifer, supports the above argument. This silicate weathering through hydrolysis reactions is favoured at Douala by the relative high temperatures and low thermal amplitude according to Segalen (1965) who showed that hydrolysis reactions are more intense and faster in humid tropical regions. Thanks to the constantly high temperature, the presence of free H^+ ions in the superficial water allows a chemical decomposition of the rock minerals.

It is worthwhile noting that the sample of Yabea identified on the Gibbs diagram in the field of rock dominance is affected by carbonate dissolution. This assertion is supported by the saturation indexes (SI) corresponding to -0.99, -1.1 and -1.5 respectively for calcite, aragonite and dolomite while for the rest of boreholes $SI_{calcite}$, $SI_{aragonite}$ and $SI_{dolomite}$ vary respectively from -2.3 to -4.9, -2.5 to -5.1 and -3.5 to -9.7. Indeed, since previous works on geology mentioned the presence of carbonate layers in the lower Pliocene, this reinforces the hypothesis that this sample corresponds to a borehole tapping a very deep part of the MP aquifer and therefore relatively old water. The dissolution phenomenon may also be enhanced by the hyper-rainy character of Douala which enables significant drainage in promoting the solubilisation of elements (Helgeson et al. 1984). Thus, the peculiar climate of Douala is a control factor of water-rocks interactions accelerating the reactions of hydrolysis and dissolution.

Besides, the water-rocks interaction reinforced by the water residence time and the hot and humid climate of Douala, another considerable control factor of groundwater chemistry is the anthropization phenomenon.

To check the influence of this phenomenon on the Mio-Pliocene aquifer of Douala, we compiled historical data on nitrates concentrations measured in 2011 (Fantong et al. 2016),

564 2014 (Emvoutou 2018), 2015 (Wirmvem et al. 2017) and 2017 (this study) during the dry
565 season at Douala. Nitrates generally well reflect the impact of human activities on the water
566 resource. Thus, regarding the urbanization trend in Douala, the high increase in population
567 and inhabitants density (Nlend et al. 2018), we expect that NO_3^- content in groundwater
568 would increase overtime. For the 2011-2017 period, maximum values show a linear variation,
569 a positive trend: from 24.0 mg/l to 245.6 mg/l. Median values evolve from 6.0 to 29.3 mg/l
570 (Fig. 12). These latter values are significantly above the global natural levels of NO_3^- in
571 groundwater (Appelo & Postma 1993). The progressive increase of nitrates in groundwater is
572 a worrying feature revealing the strong anthropogenic constrains on groundwater resource and
573 therefore the water quality decline.
574
575 Figure 12
576
577 Further, the influence of cation exchange was investigated. Like Emvoutou et al (2018), we
578 found a lack of cation exchange which is evidence that the MP aquifer is not impacted by
579 seawater intrusion. Indeed, according to Martínez & Bocanegra (2002, when sea water
580 intrudes a fresh water aquifer, cation exchange takes place and sodium is taken-up by the
581 exchanger, while Ca^{2+} is released into groundwater. Therefore, the increase in water
582 mineralization, chloride and sodium near the estuary (Fig. 9) are not linked to saline intrusion.
583 The Cl^-/HCO_3^- ratio confirms this fact; with 1.8 molar ratio (Cl^- = 94.4 mg/l) for the sample of
584 Essengue while Wirmvem et al (2017) reported that surface water at the estuary has a Cl^-
585 $/HCO_3^-$ molar ratio of 100 with approximately 5000 mg/l of Cl^-.
586 In summary, the water-rocks interactions processes can then be considered as amplified by the
587 residence time and the typical climate conditions of Douala (hot and humid). In addition, the
588 distribution of NO_3^- in boreholes, hand dug-wells and springs (Table 3) and the historical

589 evolution of this ion in groundwater suggest a strong impact of human activities on the
590 aquifer system. Further, as it has been highlighted that seawater does not intrude freshwater,
591 high levels of Cl^-, SO_4^{2-} and Na^+ would also correspond to consequences of human activities.
592 In the next section, we will evaluate the anthropogenic part in water chemistry by determining
593 the natural background and threshold values for major elements.
594

595 **4.4. Determination of natural background levels (NBL) and threshold values (TV)**

596 Background level of a substance in groundwater is defined as the concentration of a given
597 element, species or chemical substance present in solution, which is derived from natural
598 geological, biological or atmospheric sources (Edmunds et al. 2003). However, there are
599 various methods to identify NBL: hydrochemical simulation of solution in aquifers (Sellerino
600 2014), pre-selection (Coetsiers et al. 2009), component separation, probability plot and other
601 statistical methods (e.g., Sellerino 2014; Zhang et al. 2017). Among these set of methods, the
602 preselection is the simplest to approach the natural groundwater composition of an aquifer
603 when no national methodology exists for the derivation of NBL. In addition, this method is
604 the more suitable for non-expert users and all the stakeholders involved in water management.
605 The pre-selection methodology here consists in the removing samples from unknown depth,
606 samples close to the estuary (where saline intrusion could be suspected or tide influence),
607 groundwater analyses with nitrates concentrations larger than 10 mg/l, so as to remove
608 polluted samples.
609 Then the NBL will be helpful to determine the threshold values for groundwater. According
610 to Last et al (2014) TV represent a groundwater quality standard that is based on interactions
611 with aquatic and terrestrial ecosystems, interference with legitimate uses or functions of
612 groundwater, and hydro-geological characteristics including background levels. In this study

613 it was proposed to define the TV following two different cases based on the ratio between the
614 natural background level and a relevant reference value (Muller et al. 2006):
615 Case 1: NBL < REF: TV = (NBL+REF)/2
616 Case 2: NBL > REF: TV = NBL
617 REF is an appropriate reference value, defined by the World Health Organization (WHO) or
618 by any other legislation.
619 NBL and TV calculated are shown in Table 4, resulting from the application of the selected
620 methodology to the dataset. The values for NBL are presented as minimum and maximum.
621 The TV was calculated by using the maximum NBL values.
622 Table 4 shows that the concentrations in chemical elements are mostly above the NBL in
623 shallower water from hand-dug wells and springs than in deep water from boreholes. This can
624 be explained by the fact that shallow groundwater is more sensible to anthropogenic
625 influences. However, samples presenting HCO_3^- contents above the NBL are mostly observed
626 in boreholes. These samples correspond to the deepest groundwater. Since, this element is
627 only related to natural processes it is therefore clear that the deeper the groundwater flows, the
628 more the groundwater mineralization increases due to water-rocks interactions. Groundwater
629 depth should be considered in identifying geochemical processes. Likewise, as expected, the
630 majority of samples which show chemical contents above the TV are from hand-dug wells.
631 However, it is worthwhile noting, as it can be seen from Table 4, that 73% and 46% of
632 samples from boreholes have a NO_3^- above the defined NBL and TV respectively.
633 This observation implies that the aquifer pollution is probably not limited to shallower flow
634 path. Thus water from boreholes is also vulnerable to nitrate pollution. This latter appears as a
635 serious concern in term of qualitative potential of groundwater.
636 Finally, the pristine natural background value of nitrate obtained in this study for MP sands
637 (6.6 mg/l) is very close to that obtained by Zhang et al (2017) in North China plain on gravel

638 sediments. The nitrate TV (28.3 mg/l) is also similar to the one found by Coetsiers et al
639 (2009) on fluvial deposits in Flanders, Belgium. NBL and TV values obtained in this study
640 also correspond to that provided by Appelo & Postma (1993). This tends to validate the
641 accuracy of the results for the Douala region and the methodology used.
642
643
644 Table 4

5. Final discussion: proposition of a conceptual scheme of MP aquifer functioning

The present study brings out the detailed hydrogeological features characterizing an aquifer in hyper-humid region. The approach used involves hydro-climatic data, measures of potentiometric levels, stable isotopes and hydrochemistry. It is the first time that such kind of study is achieved in the Central Africa tropical humid region. The results obtained allows for the design of the hydrogeological conceptual model of the region including the structure and functioning of the aquifer system (Figure 13).

Figure 13

It has been shown that the hyper-rainy conditions lead to hyper-recharge of the aquifer approximately all the yearlong. This water then infiltrates the soil without undergoing evaporation. Mio-Pliocene groundwater flows towards the estuary supplying the main river of the region and the superficial Quaternary aquifer. Two flow paths have been identified: the shallower one is homogeneous in term of isotopes indicating a mixing between different flow paths probably due multi-level screened drillings, but heterogeneous in term of major ions chemistry thus reflecting various influences on this upper part of the aquifer. The more the water flows deeply, the more the isotope and chemical content decreases while homogenizing. Regarding the lateral flow, the mineralization generally increases from the recharge zone to the estuary. One key result is that water from the deepest part of the aquifer seems to have a relatively long residence time. The most depleted value in $\delta^{18}O$ (~ -5‰), while the weighted mean rainfall is of -2.8 $\delta^{18}O$-, the low tritium contents (0 TU) and the very low content of NO_3^- (<10 mg/l) recorded on the sample of Yabea suggest the presence of old water (over 70 years old) in the aquifer system. Thus, Mio-Pliocene aquifer gathers water recharged recently and older ones. Thanks to the estimation of NBL and TV it can be estimated that deep flow

669 path is reached at approximately 50 meters to the soil. However, as some boreholes have
670 chemical contents above the NBL or TV, it is obvious that deeper levels of the aquifer already
671 show a slight influence of anthropogenic activities on the chemistry. While NBL and TV
672 derivation is an important task for European Union (EU) Member States, it is the first time
673 that such investigation was conducted in Sub-Saharan Africa. In the implementation of
674 Integrated Water Resources Management (IWRM), well defined NBL and TV helped the EU
675 Member states to correctly assess the chemical status of ground-water bodies and to
676 implement the Groundwater Directive (Wendland et al. 2008; Preziosi et al. 2010). Indeed
677 NBL and thresholds limits constitute a basis for clean-up remediation and adequate water
678 legislation.

679 From the conceptual scheme obtained, in term of groundwater potential, the important
680 recharge of the Mio-Pliocene aquifer (linked to the hyper-humid climate) reflects the good
681 quantitative potential of the resource. This hyper-recharge also affects the groundwater
682 quality by maintaining the groundwater at a shallow level even during the dry season. Thus,
683 groundwater resource would be easily affected by contaminants at the surface. High-intensity
684 rainfall events pose a risk to shallow and poorly protected groundwater sources. This is
685 particularly an issue for unimproved dug wells and springs. Shallow groundwater levels also
686 pose a significant risk to shallow water sources in urban settings due to reduced attenuation in
687 the unsaturated zone when groundwater intersects with the base of pit latrines and sewer
688 networks (Lapworth et al. 2017). Another feature resulting indirectly from aquifer hyper-
689 recharge is the high groundwater velocity which can foster the rapid transfer of pollutants
690 within the aquifer. Thus in the light of this work, it is urgent to implement pragmatic water
691 management strategies. The groundwater recharge zones identified on the potentiometric map
692 (Fig 6) must be protected. Any activity presenting a risk of contamination of water should be
693 prohibited and managers should promote the establishment of protection perimeters around

694 the tapping points. The knowledge of lateral flow velocity could help to design security
695 distances between pollution sources and groundwater pumping points. In addition, for
696 security and sustainability of groundwater use, a legal framework must now be established for
697 groundwater abstraction especially for boreholes construction to control more efficiently the
698 exploitation of the deeper part of the aquifer since it gathers relatively old and good quality
699 water. Indeed, the paleo-groundwater in the Mio-Pliocene must be considered as a strategic
700 resource since it may be non-renewable. Therefore, the abstraction of this type of water must
701 be planned and only reserved to public authorities. Furthermore, multilevel screened wells
702 must be prohibited to avoid mixing between different flow paths. In addition, stakeholder
703 participation through local committees for environment protection should be in charge of the
704 maintenance of landfills in settlements and/or watersheds. This is essential to limit the
705 influence of human activities on the aquifer system through a better land use management.
706 Furthermore, since surface waters are intimately related to groundwater, the continuous
707 degradation of this latter would impact on the long-term the socio-ecosystem of the local
708 river.

709 Finally, beyond the critical evaluation of NBL and TV determination method, this
710 research aims at increasing consciousness in the water management authorities
711 that groundwater status assessment should be conceived as a scientific evaluation
712 procedure and not as a technical/administrative exercise to be performed using any set
713 of available data. As such, it should be supported by adequate knowledge of
714 hydrogeological setting, hydrochemical processes occurring in groundwater bodies, and
715 human activities acting overland to be progressively verified.

716 **6. Conclusion**

717 The results of this work may be extended to many porous aquifers in hyper-humid tropics.
718 Indeed, this study by highlighting specific behaviors (e.g., high recharge rate, water recycling

719 within the vadose zone through plants transpiration, high groundwater velocity, acceleration
720 of hydrolysis and dissolution reactions thanks to the hot and humid climate) of aquifers in
721 hyper-humid areas, is a contribution to a better understanding of tropical hydrology. The
722 water table fluctuation method has proven to be effective for estimating groundwater recharge
723 in a shallow water table aquifer of humid area. The estimate is consistent with that found in
724 the literature and not far to that obtained by the application of water balance method. In spite
725 of low thermal amplitude characterizing the study region, the use of water stable isotopes
726 appears as a very powerful tool to study processes affecting the transfer of rainwater to the
727 vadose zone. Stable isotopes also shown that the studied aquifer submitted to hyper-recharge
728 gathers both recent infiltrated water and paleogroundwater. While in the past they have been
729 implemented only in arid and temperate climates, this study constitutes a new testimony of
730 the possibilities offered by isotope techniques in hydrogeological studies in humid countries.

731 Substantial information on groundwater recharge, groundwater flow conditions, groundwater
732 chemistry added to the determination of NBLs and TV will be helpful to elaborate future
733 groundwater management strategies, especially in developing countries of Africa. Indeed, the
734 limited waste management and high intrinsic vulnerability lead to urban aquifer (as Mio-
735 Pliocene at Douala) highly impacted by chemical loading posing a clear health risk to users.
736 NBLs defined are essential when considering deterioration of groundwater quality, and in
737 addition these values can be a basis when restoring groundwater quality. Threshold values
738 should be incorporated in formulating new water quality standards for groundwater in
739 Cameroon, and more generally in sub-Saharan Africa. More generally, this approach provides
740 useful information for the establishment of a new water supply scheme with respect to the
741 climate specificity and the urban context.

742 **Authorship contribution statement**

743 **B. Nlend:** Conceptualization, Investigation, Methodology, Resources, Writing - original and
744 revised manuscripts. **H. Celle-Jeanton:** Conceptualization, Methodology, Resources,
745 Supervision, Writing - review & editing. **F. Huneau:** Conceptualization, Investigation,
746 samples analyses, Supervision, Writing- review & editing. **E. Garel:** samples analyses,
747 Methodology, Writing - review & editing. **S. Boum-Nkot:** Conceptualization, Writing -
748 review & editing. **J. Etame:** Methodology & supervision.

749

750 **Acknowledgments**

751 This paper constitutes a part PhD study of the first author who was supported by a doctoral
752 scholarship from the French Ministry of Foreign Affairs. The authors thank the French
753 Embassy to the Republic of Cameroon for all mobility facilities provided during the study.

754
755
756
757 **References**
758

759 Adimalla A (2018) Spatial distribution, exposure, and potential health risk assessment from
760 nitrate in drinking water from semi-arid region of South India. *Human and Ecological Risk*
761 *Assessment*. 10.1080/10807039.2018.1508329.

762 Allen RG, Howell TA, Pruitt WO, Walter IA, Jensen ME (eds) (1991) Lysimeters for
763 evapotranspiration and environmental measurements. In: Proc *Int Symp on Lysimetry,*
764 *American Society of Civil Engineers*, New York, 444 pp

765 Allison GB, Gee GW, Tyler SW (1994) Vadose-Zone Techniques for Estimating Groundwater
766 Recharge in Arid and Semiarid Region. *Soil Sci. Soc. Am. J*. 58:6-14

767 Appelo CAJ, Postma D (1993) Geochemistry, Groundwater and Pollution. 3rd Edn., AA
768 Balkema, Rotterdam, Netherlands, ISBN:9789054101062, Pages: 536.

769 Barbeta A & Peñuelas J (2017) Relative contribution of groundwater to plant transpiration
770 estimated with stable isotopes. *Scientific Reports*, 7: 10580, DOI:10.1038/s41598-017-09643x

771 Barnes CJ, Allison GB (1988) Tracing of water movement in the unsaturated zone using stable
772 isotopes of hydrogen and oxygen. *J. Hydrol*. 100: 143-176.

773 Bourgeois M (1977) Etude hydrogéologique d'orientation pour le captage d'eau minérale au
774 Cameroun. Rap, BRGM 77 AGE 013.

775 Blavoux B (1978) Etude du cycle de l'eau au moyen de l'oxygène-18 et du tritium. Possibilités
776 et limites de la méthode des isotopes du milieu en hydrologie de la zone tempérée ». Thèse
777 doctorat, Univ. Paris VI, 333 p.

778 Braune E, Xu Y (2009) The Role of Ground Water in Sub-Saharan Africa *Ground Water*, vol.
779 48. Pp 229–238, 2.

780 Coetsiers M, Blaser P, Martens K, Walraevens K (2009) Natural background levels and
781 threshold values for groundwater in fluvial Pleistocene and Tertiary marine aquifers in
782 Flanders, Belgium. *Environ Geol* 57:1155–1168; DOI 10.1007/s00254-008-1412-z

783 Craig H (1961) Isotopic variation in meteoric waters. *Science* 133, 1702–1703

784 Dansgaard W (1964) Stable isotopes in precipitation. *Tellus* 16 (4), 436–468.

785 Dar FA, Perrin J, Ahmed S, Narayana AC, Riotte J (2014) Hydrogeochemical characteristics of
786 Karst Aquifer from a semi-arid region of Southern India and impact of rainfall recharge on
787 groundwater chemistry. *Arab J Geosci* 8(5):2739–2750. doi:10.1007/s12517-014-1440-9

788 Din Ndongo (2001) Mangrove du Cameroun, statut écologique et perspectives de gestion
789 durable. Thèse ès sci, Univ. Yaoundé I, 255p.

790 Djebebe-Ndjiguim CL, Huneau F, Denis A, Foto E, Moloto-A-Kenguemba G, Celle-Jeanton H,
791 Garel E, Jaunat J, Mabingui J, Le Coustumer P (2014). Characterization of the aquifers of the
792 Bangui urban area as an alternative drinking water supply resource. *Hydrol. Sci. J*. 58, 1760–
793 1778. http://dx.doi.org/10.1080/02626667.2013.826358.

794 Dumort JD (1968) Notice explicative sur la feuille Douala-Ouest carte géologique de
795 reconnaissance (1/500000). Publication Direction des Mines et de la Géologie du Cameroun,
796 69p

797 Edmunds WM, Shand P, Hart P, Ward RS (2003) The natural (baseline) quality of groundwater:
798 a UK pilot study. *Sci Total Environ* 310:25–35

799 Emvoutou H (2018) Fonctionnement hydrodynamique du système aquifère du bassin
800 sédimentaire côtier dans la ville de Douala. Apports des outils géochimiques, géostatistiques
801 et isotopiques. *PhD thesis*, Université cheikh Anta Diop de Dakar, Senegal; 267p.

802 Fantong WY, Fouepe AT, Ketchemen-Tandia B, Kuitcha D, Ndjama J, Fouepe TA, Takem GE,
803 Issa, Wirmvem MJ, Bopda Djomou SL, Ako AA, Nkeng GE, Kusakabe M, Ohba T (2016)
804 Variation of hydrogeochemical characteristics of water in surface flows, shallow wells and
805 boreholes in the coastal city of Douala (Cameroon). *Hydrol. Sci. J*.
806 http://dx.doi.org/10.1080/02626667201611737789

807 Feumba R (2015) Hydrogéologie et évaluation de la vulnérabilité des nappes dans le bassin
808 versant de Bessekè (Douala-Cameroun). *Thèse de Doctorat PhD*, Département de Sciences de
809 la Terre, Faculté des Sciences. Université de Yaoundé I, 226p.

810 Feumba R, Ngounou Ngatcha B, Tabue Youmbi JGh, Ekodeck GE (2011) Relationship between
811 climate and groundwater recharge in the Besseke Watershed (Douala-Cameroon). *J. Water*
812 *Resour. Prot*, 3, 607–619. http://dx.doi.org/10.4236/ jwarp201138070. Published Online
813 August 2011 (http://wwwSciRPorg/journal/jwarp).

814 Fontes J-Ch (1983) Dating of groundwater. In: Guidebook on Nuclear Techniques in
815 Hydrology. *Technical Report Series* No. 91. IAEA. Vienna.

816 Fosberg FR, Garnier BJ, & Küchler AW (1961) Delimitation of the Humid Tropics.
817 *Geographical Review*, Vol. 51, No. 3, pp. 333-347. http://www.jstor.org/stable/212781.

818 Foster SSD (1993) Groundwater conditions and problems characteristic of the humid tropics
819 Hydrology of Warm Humid Regions. *Proceedings of the Yokohama Symposium*, July 1993
820 216, 1993 (lAHSP0olno), 433-449.

821 Foster SSD & Chilton PJ (1993) Groundwater systems in the humid tropics. In: UNESCO-IHP
822 Humid Tropics Book. Cambridge University Press

823 Foster SSD, Bousquet A, Furey S. (2018) Urban groundwater use in tropical Africa – a key
824 factor in enhancing water security? *Water Policy* 20, 982–994.

825 Healy RW, Cook PG (2002) Using groundwater levels to estimate recharge. *Hydrogeol J* 10:91
826 109

827 Helgeson HC, Murphy WM, Aagaard P (1984) Thermodynamic and kinetic constraints on
828 reactionrates among minerals and aqueous solutions, II. Rateconstants, effective surface area,
829 and the hydrolysis of feldspar. *Geochim. Cosmochim. Acta*, 48: 2405-2432

830 Helm C (2009) Quantification des flux sédimentaires anciens à l'échelle d'un continent : le cas
831 de l'Afrique au Méso-Cénozoïque. *PhD thesis* (In French), Université de Rennes 1, 309p

832 Huneau F, Dakoure D, Celle-Jeanton H, Vitvar T, Ito M, Compaore NF, Traore S, Jirakova H,
833 Le Coustumer P (2011) Flow pattern and residence time of groundwater within the south-
834 eastern Taoudeni sedimentary basin (Burkina Faso Mali). *J. Hydrol*. 409. 423–439

835 IAEA/WMO (2019) Global Network of Isotopes in Precipitation. The GNIP Database
836 accessible at: https://nucleus.iaea.org/wiser.

837 Jiráková H, Huneau F, Celle-Jeanton H, Hrkal Z, Le Coustumer P (2011) Insights into
838 palaeorecharge conditions for European deep aquifers. *Hydrogeology Journal* 19 (8), 1545-
839 1562

840 Johnson AI (1967). Specifc yield: compilation of specific yields for various materials. *US*
841 *Geological Survey Water-Supply Paper* 1662-D.

842 Keesari T, Ramakumar KL, Prasad MBK. et al (2015) Microbial Evaluation of Groundwater
843 and its Implications on Redox Condition of a Multi-Layer Sedimentary Aquifer System.
844 *Environ. Process*. 2, 331–346 (2015). https://doi.org/10.1007/s40710-015-0067-5

845 Ketchemen-Tandia B (2011) Déterminants hydrogéologiques de la complexité dusystème
846 aquifère du bassin sédimentaire de Douala (Cameroun). University of Cheick Anta Diop
847 *Thesis diss* (in French) 211 p.

848 Ketchemen-Tandia B, Ngo Boum S, Ebonji SCR, Wonkam C, Nkoue Ndong GR, Huneau F,
849 Celle-Jeanton H (2011) Stable isotopic composition of rainfall from Western Cameroon
850 IAEA, *Symp on Isotopes in Hydrol, Marine Ecosystems, and Climate Change Studies* in
851 Monaco Monaco.

852 Ketchemen-Tandia B, Boum-Nkot SN, Ebondji SR, Nlend BY, Emvoutou H, Nzegue O (2017)
853 Factors Influencing the Shallow Groundwater Quality in Four Districts with Different
854 Characteristics in Urban Area (Douala, Cameroon). *Journal of Geoscience and Environment*
855 *Protection*. 5. 99-120. https://doi.org/10.4236/gep.2017.58010

856 Kopa NKA, Likeng HDJ, Nono A (2012) Hydrodynamique et qualité des eaux souterraines dans
857 le bassin sédimentaire de Douala (Cameroun): Cas des aquifères sur formations quaternaires
858 et tertiaires. *Int J Biol Chem Sci* 6(4):1874–1894

859 Kotchoni DOV, Vouillamoz JM, Lawson FMA, Adjomayi Ph, Boukari M, Taylor RG (2019)
860 Relationships between rainfall and groundwater recharge in seasonally humid Benin: a

comparative analysis of long-term hydrographs in sedimentary and crystalline aquifers. *Hydrogeology Journal*, 27:447–457. https://doi.org/10.1007/s10040-018-1806-2

Lakshmanan E, Kannan R, Kumar MS (2003) Major ion chemistry and identification of hydrogeochemical processes of groundwater in a part of Kancheepuram district, Tamil Nadu, India. *Environmental Geosciences* 10:157–166.

Lapworth DJ, Nkhuwa DCW, Okotto-Okotto J, Pedley S, Stuart ME, Tijani MN, Wright J (2017) Urban groundwater quality in sub-Saharan Africa: current status and implications for water security and public health. *Hydrol. J.* 25. 1093–1116. http:// dx.doi.org/10.1007/s10040-016-1516-6

Last GW, Murraya CJ, Botta Y, Browna CF (2014) Threshold Values for Identification of Contamination Predicted by Reduced-Order Models. Energy Procedia 63 (2014) 3589 – 3597; doi: 10.1016/j.egypro.2014.11.389.

Lee RW, Strickland DJ (1988) Geochemistry of groundwater in Tertiary and Cretaceous sediments of the south-eastern coastal plain in eastern Georgia, South Carolina, and south-eastern North Carolina. *Water Resources Research* 24:291–303

Lienou G, Sighomnou L, Sigha Nkamdjou L, Malou R, Saos J-L (1999) Caractérisation des relations eaux de surface - eaux souterraines en milieu tropical sec : exemple du bassin de la nema (Sine Saloum, Senegal). *Sud Sciences and Technologies*, N°3.

Lu X, Liang LL, Wang L, Jenerette GD, McCabe MF, & Grantz DA (2017). Partitioning of evapotranspiration using a stable isotope technique in an arid and high temperature agricultural production system. *Agricultural Water Management*, 179, 103–109. https://doi.org/10.1016/j.agwat.2016.08.012

Mafany GT (1999) Impact of the geology and seawater intrusion on groundwater quality in Douala. Thesis (M.Sc.). University of Buea, 252

885 Manga CS (2008) Stratigraphy, structure and prospectivity of the Southern onshore Douala
886 Basin, Cameroon- Central Africa. *Africa Geoscience Review*, 13-37

887 Marechal JC, Dewandel B, Ahmed S, Galeazzi L, Zaidi FK (2006) Combined estimation of
888 specific yield and natural recharge in a semi-arid groundwater basin with irrigated agriculture.
889 *J Hydrol* 329:281–293

890 Martínez DE & Bocanegra EM (2002) Hydrogeochemistry and cation-exchange processes in the
891 coastal aquifer of Mar Del Plata, Argentina. Hydrogeol. J. 10, 393–408.

892 Medeiros PV, Marcuzzo FFN, Youlton C, Wendland E (2012) Error autocorrelation and linear
893 regression for temperature-based evapotranspiration estimates improvement. *J Am Water Res*
894 *Assoc*, 48:297-305.

895 Mohan C, Western A, Wei Y, Saft M (2018) Predicting groundwater recharge for varying land
896 coverand climate conditions – a global meta-study. *Hydrol. Earth Syst. Sci*., 22, 2689–2703.
897 https://doi.org/10.5194/hess-22-2689-2018

898 Moulin M (2003) Etude géologique et géophysique dees marges continentales passives :
899 exemples du Zaïre et de l'Angola, *PhD Thesis*, Université de Bretagne Occidentale, Brest,
900 France.

901 Muller D, Blum A, Hookey J, Kunkel R, Scheidleder A, Tomlin C, Wendland F (2006) Final
902 proposal of a methodology to set up groundwater threshold values in Europe. Specific
903 targeted EU research project BRIDGE (contract No SSPI-2004-006538)- report D18.
904 www.wfd-bridge.net

905 Ndomè EPE (2010) Minéralogie, géochimie et applications géotechniques des produits
906 d'altération sur roches sédimentaires de Douala. *Thèse de Doctorat PhD*, Département des
907 Sciences de la Terre, Faculté des Sciences, Université de Yaoundé I, 222 p + annexes.

908 Ngo Boum NS, Ketchemen-Tandia B, Ndje Y, Emvoutou H, Ebonji CR, Huneau F (2015)
909 Origin of mineralization of groungwater in the Bassa watershed (Douala-Cameroon). *J*
910 *Hydrogeol Hydrol Eng*. 4:1–9

911 Nguene FR, Tamfu S, Loule JP, Ngassa C (1992) Paleoenvironment of the Douala and Kribi /
912 Campo sub basins in Cameroon West Africa. *Géologie Africaine: coll*, Libreville, Recueil des
913 communic, 6-8 may 1991.6 fig.ISSNJ 010181- 0901-ISBN2-901026-34.6

914 Ngueutchoua G (1996) Etude des faciès et environnements sédimentaires du quaternaire
915 supérieur du plateau continental camerounais. *Thèse de Doctorat* Univ. Perpignan4,
916 Perpignan, 288 p.

917 Njike Ngaha PR (1984) Contribution à l'étude géologique, stratigraphique et structurale de la
918 bordure du basin atlantique du Cameroun. *Thèse 3ème cycle*, Univ. Yaoundé, 131p

919 Njike Ngaha PR, Bachirou MC, Bitom D (2014) Paleogeographic Evolution of the Eastern Edge
920 of the Douala Basin from Early Cenomanian to Turonian. *The Open Geology Journal*, 8, 124-
921 141

922 Njoh OA, Essien JA, Tembi A (2014) Albian – Turonian palynomorphs from the Mundeck and
923 Logbadjeck Formations, Ediki River, north-western part of the Douala sub-basin, Cameroon.
924 *Sciences Technologies et Development*, Vol 15. pp 66-77

925 Njoh OA, Petters SW (2014) Preliminary investigation of Late Turonian-Early Campanian
926 shallow marine foraminifera of the Mungo River/Logbadjeck Formation. NW Douala Basin.
927 Cameroon. *Journal of African Earth Sciences* 99, 442–451, 1 (2), 51–63.
928 http://dx.doi.org/10.1016/j.jafrearsci.2013.11.003

929 Nlend B, Celle-Jeanton H, Huneau F, Ketchemen-Tandia B, Fantong WY, Ngo Boum-Nkot S,
930 Etame J (2018) The impact of urban development on aquifers in large coastal cities of West
931 Africa: Present status and future challenges, *Land Use Policy*, Volume 75, Pages 352-363,

ISSN 0264-8377, https://doi.org/10.1016/j.landusepol.2018.03.007. (http://www.sciencedirect.com/science/article/pii/S026483771830125X)

Nlend B, Celle-Jeanton H, Risi C, Pohl B, Huneau F, Ngo Boum-Nkot S, Seze G, Roucou P, Camberlin P, Etame J, Ketchemen-Tandia B (2020) Identifcation of processes that control the stable isotope composition of rainwater in the humid tropical West-Central Africa. *Journal of Hydrology*, 584. https://doi.org/10.1016/j.jhydrol.2020.124650

Obuobie E, Diekkrueger B, Agyekum W, Agodzo S (2012) Groundwater level monitoring and recharge estimation in the White Volta River basin of Ghana. *Journal of African Earth Sciences*, Volumes 71–72, Pages 80-86, ISSN 1464-343X. https://doi.org/10.1016/j.jafrearsci.2012.06.005.

Olivry J-C (1986) Fleuves et rivières du Cameroun. Paris: Collection "Monographies hydrologiques ORSTOM", p 781

Onguene R, Pemha E, Lyard F, Du-Penhoat Y, Nkoue G, Duhaut T, Njeugna E, Marsaleix, P, Mbiake R, Jombe S, Allain D (2015) Overview of Tide Characteristics in Cameroon Coastal Areas Using Recent Observations. *Open Journal of Marine Science*. 5. 81-98. doi: 10.4236/ojms.2015.51008.

Ouali A, Mudry J, Mania J et al (1999). Present recharge of an aquifer in a semi-arid region: an example from the Turonian limestones of the Errachidia basin, Morocco. *Environmental Geology* 38: 171. https://doi.org/10.1007/s002540050413

Penna D, Stenni B, Sanda M, Wrede S, Bogaard TA, Gobbi A, Borga M, Fischer BMC, Bonazza M, Charova Z (2010) On the reproducibility and repeatability of laser absorption spectroscopy measurements for δ^2H and $\delta^{18}O$ isotopic analysis. *Hydrol. Earth Syst. Sci. Discuss*, 7. 2975–3014. www.hydrol-earth-syst-sci-discuss.net/7/2975/2010/doi:10.5194/hessd-7-2975-2010

956 Piccinini L, Fabbri P, Pola M (2016) Point dilution tests to calculate groundwater velocity: an
957 example in a porous aquifer in NE Italy. *Hydrol Sci J* 61(8):1512–1523.
958 https://doi.org/10.1080/02626667.2015.1036756

959 Preziosi E, Giuliano G, Vivona R (2010) Natural background levels and threshold values
960 derivationfor naturally As, V and F rich groundwater bodies: a methodological case study in
961 Central Italy. Environ Earth Sci; 61:885–897DOI 10.1007/s12665-009-0404-y

962 Rahmani SEA, Chibane B, Boucefiene A (2017) Groundwater recharge estimation in semi-arid
963 zone: a study case from the region of Djelfa (Algeria). *Appl Water Sci*, 7:2255–2265 DOI
964 10.1007/s13201-016-0399-y

965 Rajmohan N, Elango L (2004) Identification and evolution of hydrogeochemical processes in
966 the groundwater environment in an area of the Palar and Cheyyar River basins, Southern
967 India. *Environmental Geology* 46:47–61

968 Regnoult JM (1986) Synthèse Géologique du Cameroun DMG. Yaoundé; 199 p

969 Rey N, Rosa E, Cloutier V, Lefebvre R (2017) Using water stable isotopes for tracing surface
970 and groundwater flow systems in the Barlow-Ojibway Clay Belt, Quebec. *Canada. Canadian*
971 *Water Resources Journal / Revue canadienne des ressources hydriques*. DOI:
972 10.1080/07011784.2017.1403960

973 Risi C, Noone D, Frankenberg C, Worden J (2013) Role of continental recycling in intra-
974 seasonal variations of continental moisture as deduced from model simulations and water
975 vapor isotopic measurements. *Water Resour. Res*. 49, 4136–4156. https://
976 doi.org/10.1002/wrcr.20312.

977 Saghir J, Santoro J (2018) Urbanization in Sub-Saharan Africa. Center for Strategic &
978 International Studies Report, Washington, DC, USA. www.csis.org

979 Sami K (1992) Recharge mechanisms and geochemical processes in a semi-arid sedimentary
980 basin, Eastern Cape, South Africa. *Journal of Hydrology*, 139 (1992) 27-48

981 Scanlon BR, Healy RW, Cook PG (2002) Choosing appropriate techniques for quantifying
982 groundwater recharge. *Hydrogeol. J*. 10, 18–39.

983 Scanlon BR, Keese KE, Flint AL, Flint LE, Gaye CB, Edmunds W, Simmers I (2006) Global
984 synthesis of groundwater recharge in semiarid and arid regions. *Hydrological Processes*, 20,
985 3335–3370.

986 Segalen P (1965) Les produits alumineux dans les sols de la zone tropicale humide. *Cah.*
987 *ORSTOM*, sér. PédoZ., vol. III, no 3, pp. 179-205.

988 Segalen P (1967) Les sols et géomorphologie du Cameroun. *Cahier ORSTOM*, sér. Péd. Vol V,
989 n°2 Pp 137–180.

990 Sellerino M (2014) Methods of determination ofnatural background levels in groundwater: a
991 review. The definition of natural background levels (NBLs) in groundwater and soils –Case
992 studies in Italy and Portugal. Implementation of eco-compatible protocols for agricultural soil
993 remediation in Litorale Domizio-Agro Aversano NIPS. Naples, 26th February, 2014

994 SNH/UD (2005) Synthèse sur le bassin du Rio Del Rey et sur le bassin de Douala/Kribi-Campo.
995 Rapport interne. 14p.

996 State of the Tropics (2014) State of the Tropics 2014 report. James Cook University, Cairns,
997 Australia.

998

999 Takem GE, Kuitcha D, Ako AA, Mafany GT, Takounjou-Fouepe A, Ndjama J, Ntchancho R,
1000 Ateba BH, Chandrasekharam D, Ayonghe SN (2010) Acidification of shallow groundwater in
1001 the unconfined sandy aquifer of the city of Douala. Cameroon. Western Africa: implications

for groundwater quality and use. *Environ. Earth Sci*. http://dx.doi.org/10.1007/s12665-015-4681-3

Tatou RD, Kabeyene VK, Mboudou GE (2017). Multivariate Statistical Analysis for the Assessment of Hydrogeochemistry of Groundwater in Upper Kambo Watershed (Douala Cameroon). *Journal of Geoscience and Environment Protection*, 5. 252-264. https://doi.org/10.4236/gep.2017.53018

Tchiadeu G, Olinga JM (2012) La ville de douala : entre baisse des précipitations et hausse des températures. *25ème Colloque de l'Association Internationale de Climatologie*, Grenoble, France. https://www.academia.edu/14078372/LA_VILLE_DE_DOUALA_ENTRE_BAISSE_DES_PR%C3%89CIPITATIONS_ET_HAUSSE_DES_TEMP%C3%89RATURES

UNESCO (1990) Problèmes de l'eau propres aux zones tropicales humides et autres régions humides chaudes. https://unesdoc.unesco.org/in/rest/annotationSVC/DownloadWatermarkedAttachment/attach_import_32d07e35-5ea5-4fe2-9ad7-5a83c80a70fc?_=017765mulo.pdf

UNESCO (2000) A final remark on ground water in the humid tropics. http://www.bvsde.paho.org/bvsacd/cd56/hydrology/cap4.pdf

Wendland F, Berthold G, Blum C, Elsass P, Fritsche J-G, Kunkel R, Wolter R (2008) Derivation of natural background levels and threshold values for groundwater bodies in the Upper Rhine Valley (France, Switzerland and Germany). Desalination, Volume 226, Issues 1–3, 25 June 2008, Pages 160-168; https://doi.org/10.1016/j.desal.2007.01.240.

Wirmvem MJ, Ohba T, Anye Nche L, Tchakam Kamtchueng B, Kongnso WE, Mimba ME, Bafon TG, Yaguchi M, Takem GE, Fantong WY, Ako AA (2017) Effect of diffuse recharge

1025 and wastewater on groundwater contamination in Douala Cameroon *Environ. Earth Sci*. 76.
1026 354. http://dx.doi.org/10.1007/s12665-017- 6692-8.

1027 Wohl E, Barros A, Brunsell N, Chappell NA, Coe M, Giambelluca T, Goldsmith S, Harmon R,
1028 Hendrickx JMH, Juvik J, McDonnell J , Ogden F (2012) The hydrology of the humid tropics.
1029 *Nature Climate Change*, Vol 2. DOI: 10.1038/NCLIMATE1556

1030 WHO (2011) Guidelines for Drinking Water Quality, 4th ed. Geneva, Switzerland: World
1031 Health Organization.

1032 Yang Y, Lerner DN, Barrett MH, Tellam JH (1999) Quantifcation of groundwater recharge in
1033 the city of Nottingham. *UK. Environ. Geol*., 38,183–198.

1034 Zhang Y, Chen Z, Sun J, Wang J (2017) Natural background levels of chemical components in
1035 groundwater of Hutuo River catchment area, North China Plain. *Environmental Forensics*,
1036 18:1, 62-73, DOI: 10.1080/15275922.2016.1263904

1037 Zogning A (1987) - Les formations superficielles latéritiques dans la région de Douala :
1038 morphologie générale et sensibilité aux activités humaines. In: *Séminaire régional sur les*
1039 *latérites : sols, matériaux, minerais*: sessions 1 et 3. Paris: ORSTOM, p. 289-303
1040

List of Figures

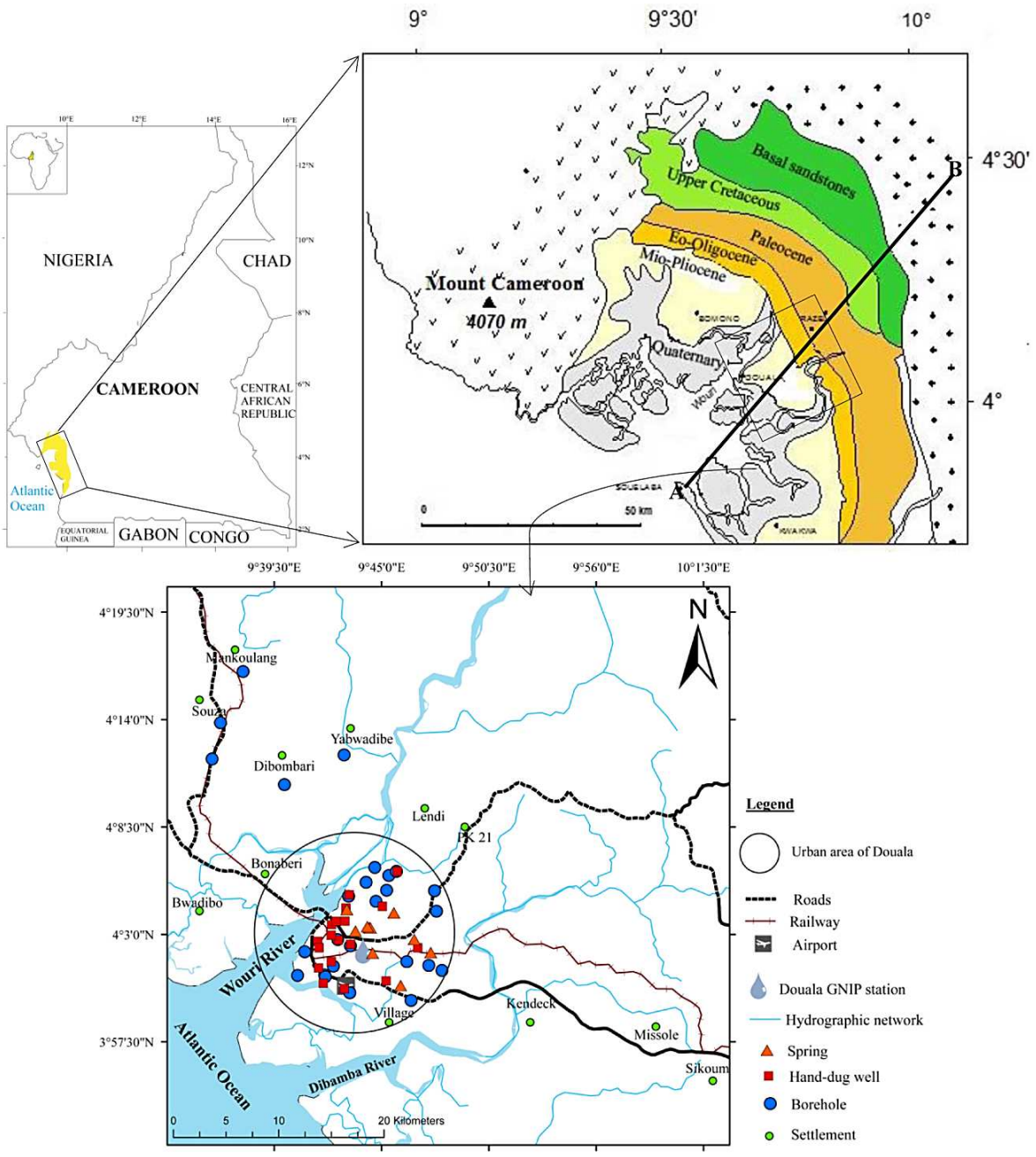

Fig. 1 Maps of the study area showing the geology of the Douala basin and the location of the sampling points. The cut line A-B refers to geological cross section presented in Fig. 3.

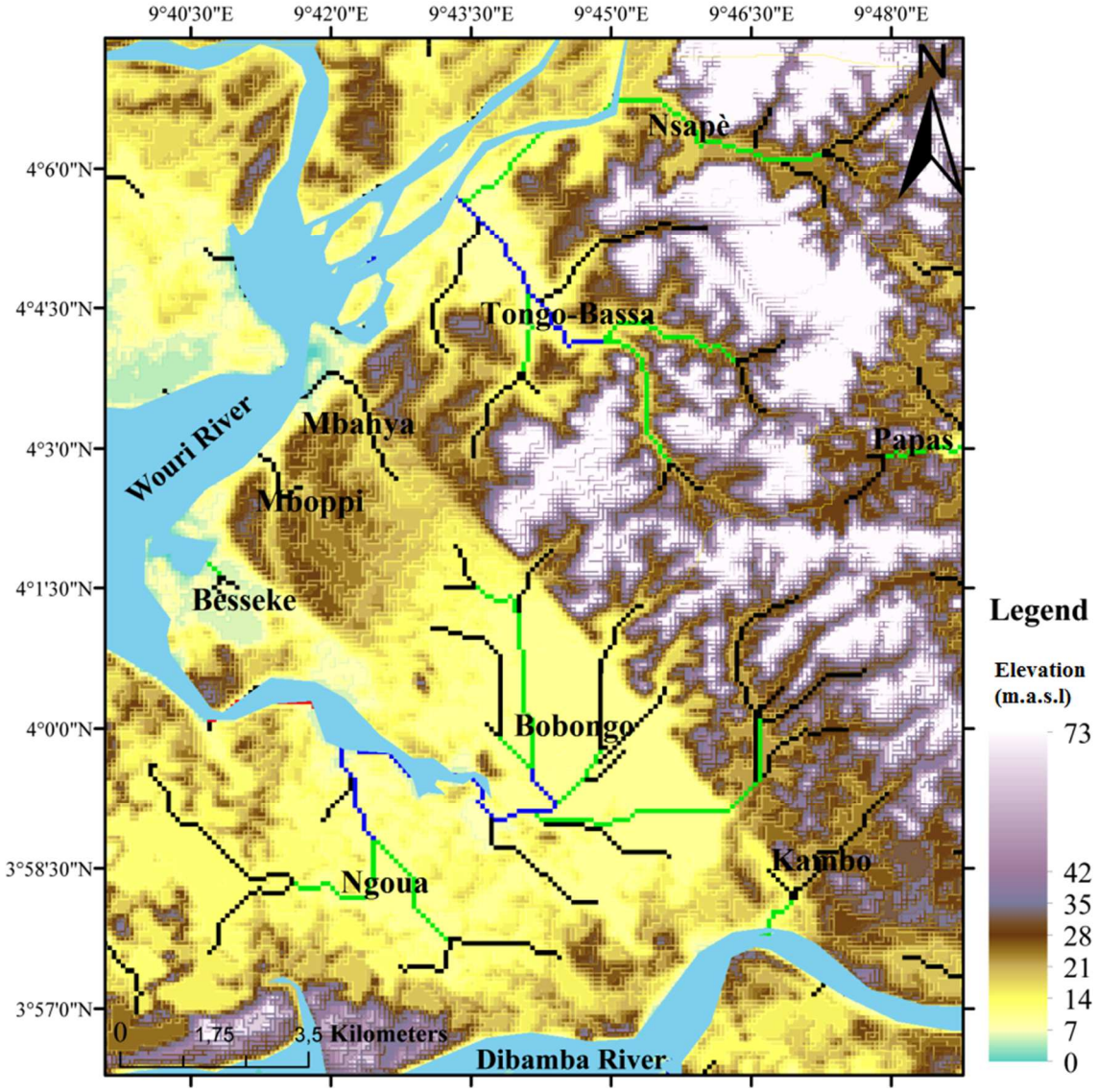

Fig. 2 Hydrographic network of the Douala megacity region and topography of the area (meters a.s.l.)

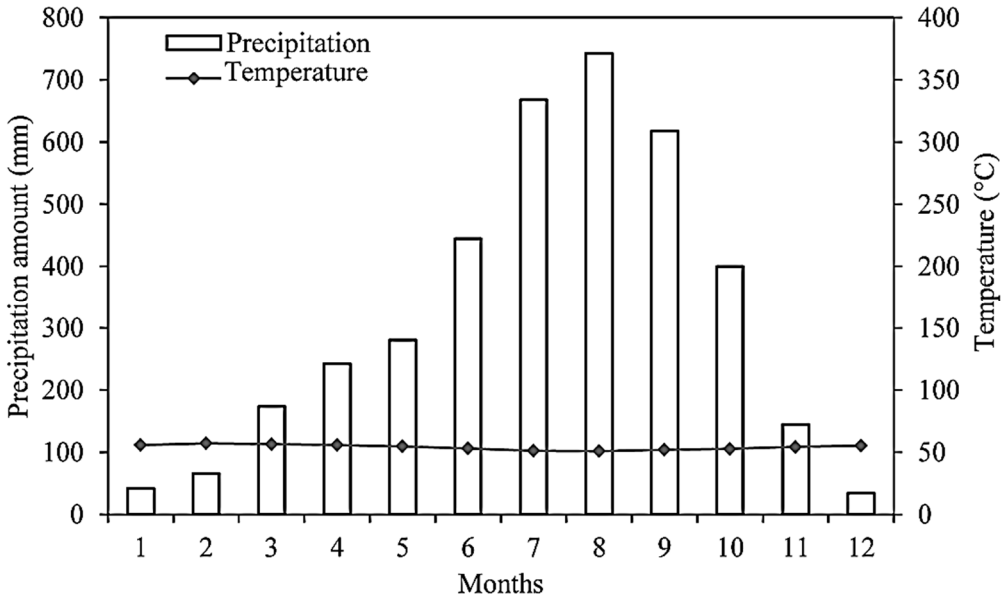

Fig. 3 Ombrothermic diagram of the region of Douala. Mean monthly variations of rainfall amounts (1951-2016) and air temperatures (1971-2016) were recorded at the meteorological station of Douala.

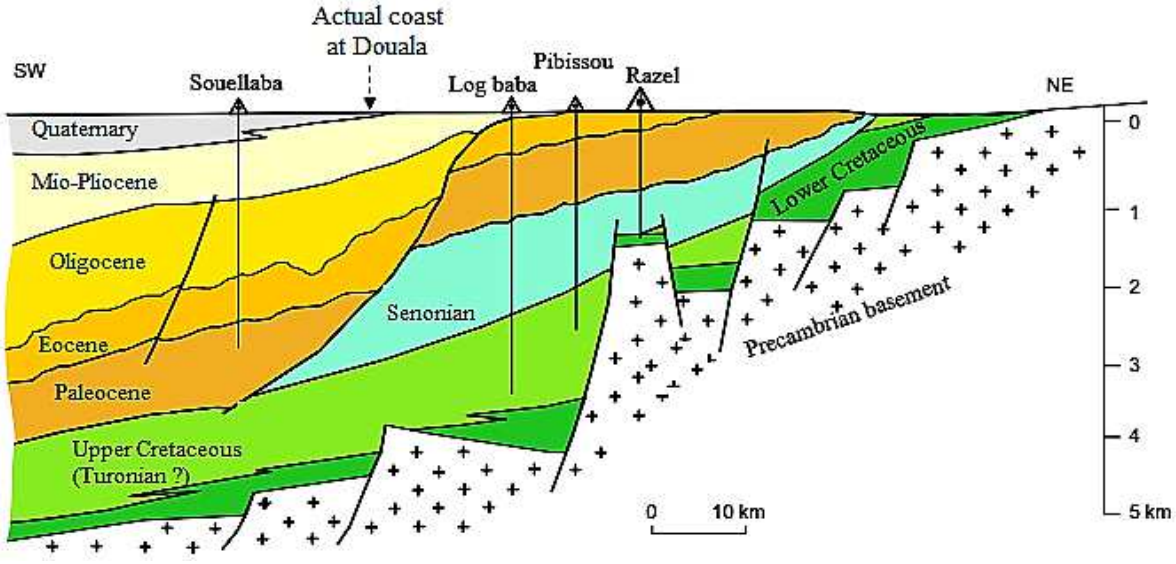

Fig. 4 Geological cross section through the Douala sedimentary basin (Regnoult 1986). The corresponding cut line is plotted on Figure 1.

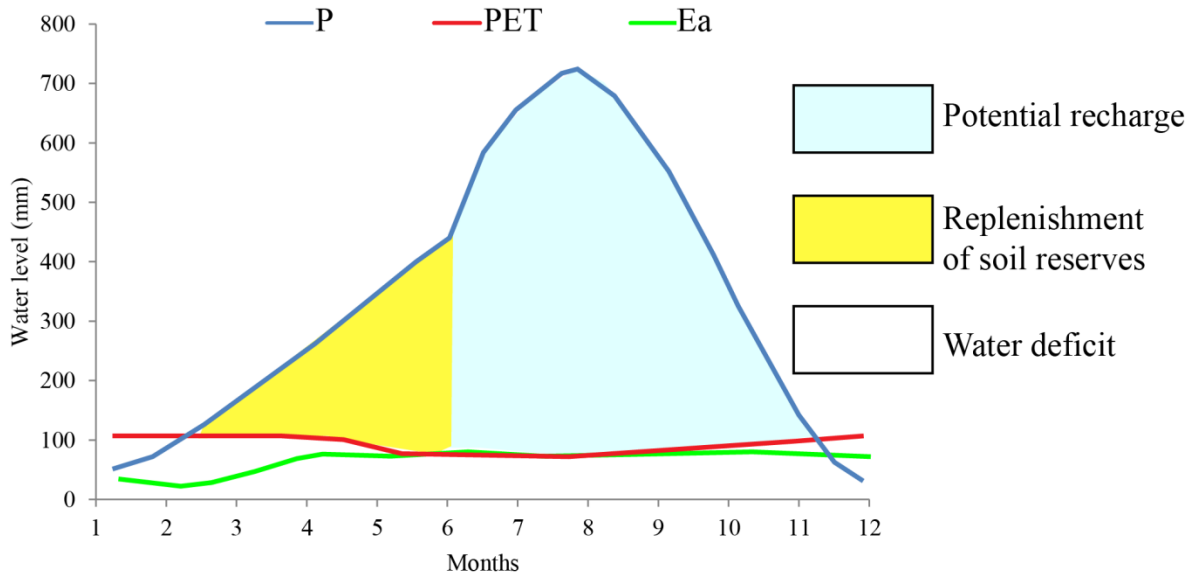

Fig. 5 Water balance in the region of Douala

P = Precipitation, PET = Potential evapotranspiration, Ea = Actual evapotranspiration

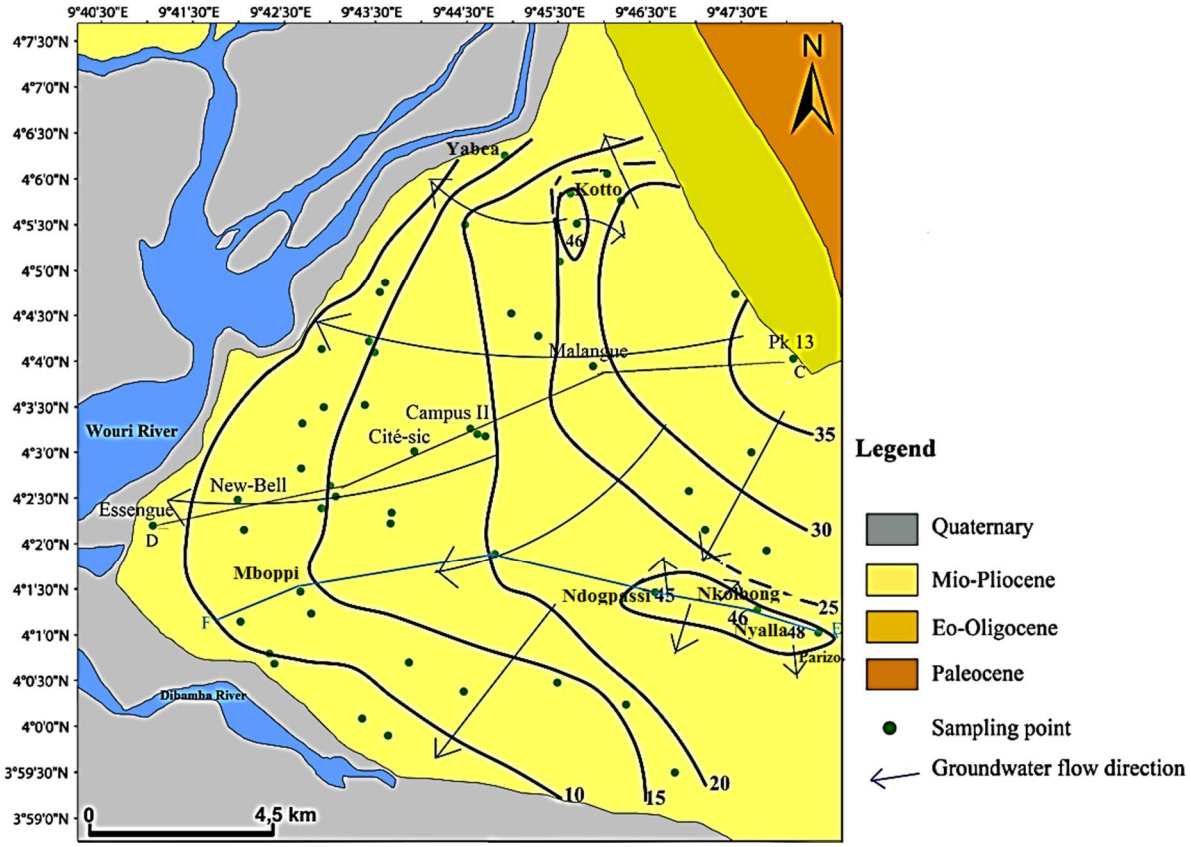

Fig. 6 Potentiometric map of the Mio-Pliocene aquifer in Douala (Cameroon) in February 2017. The locations of Nkolbong and Parizo refer to Nyalla.

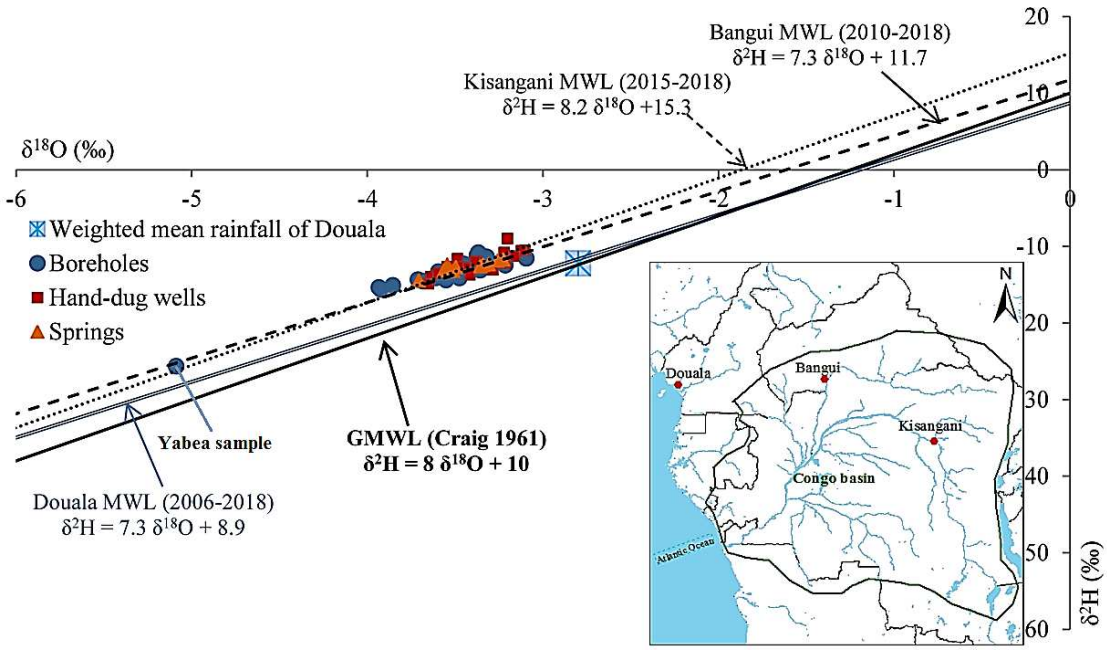

Fig. 7 $\delta^{18}O$ vs $\delta^{2}H$ diagram. Groundwater samples are reported as well as the Global Meteoric Water line (Craig 1961), the Local Meteoric Water Line and the Bangui and Kisangani water lines (IAEA/WMO 2019).

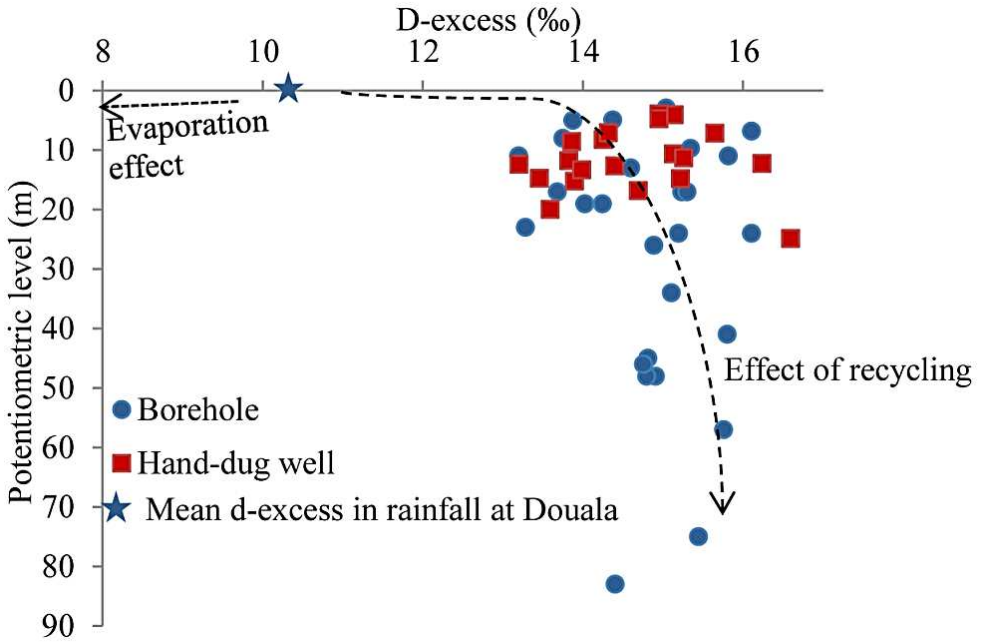

Fig. 8 Deuterium excess (D-excess) in groundwater *versus* potentiometric level. The mean values of D-excess in rainwater at Douala are also plotted.

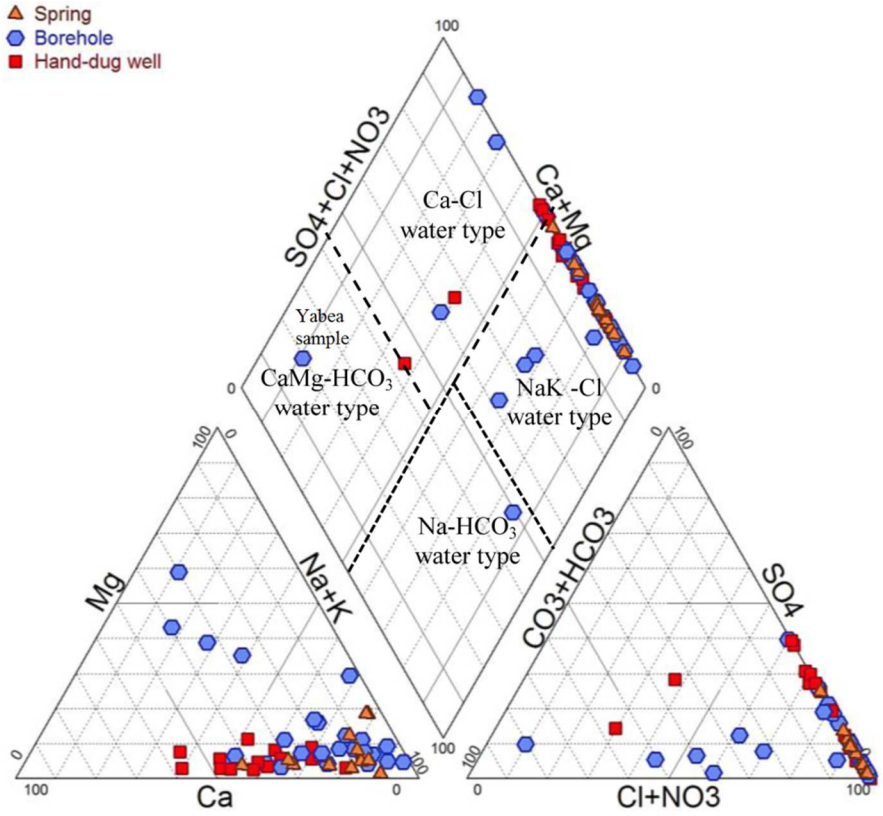

Fig. 9 Piper diagram of Mio-Pliocene groundwater at Douala (Cameroon)

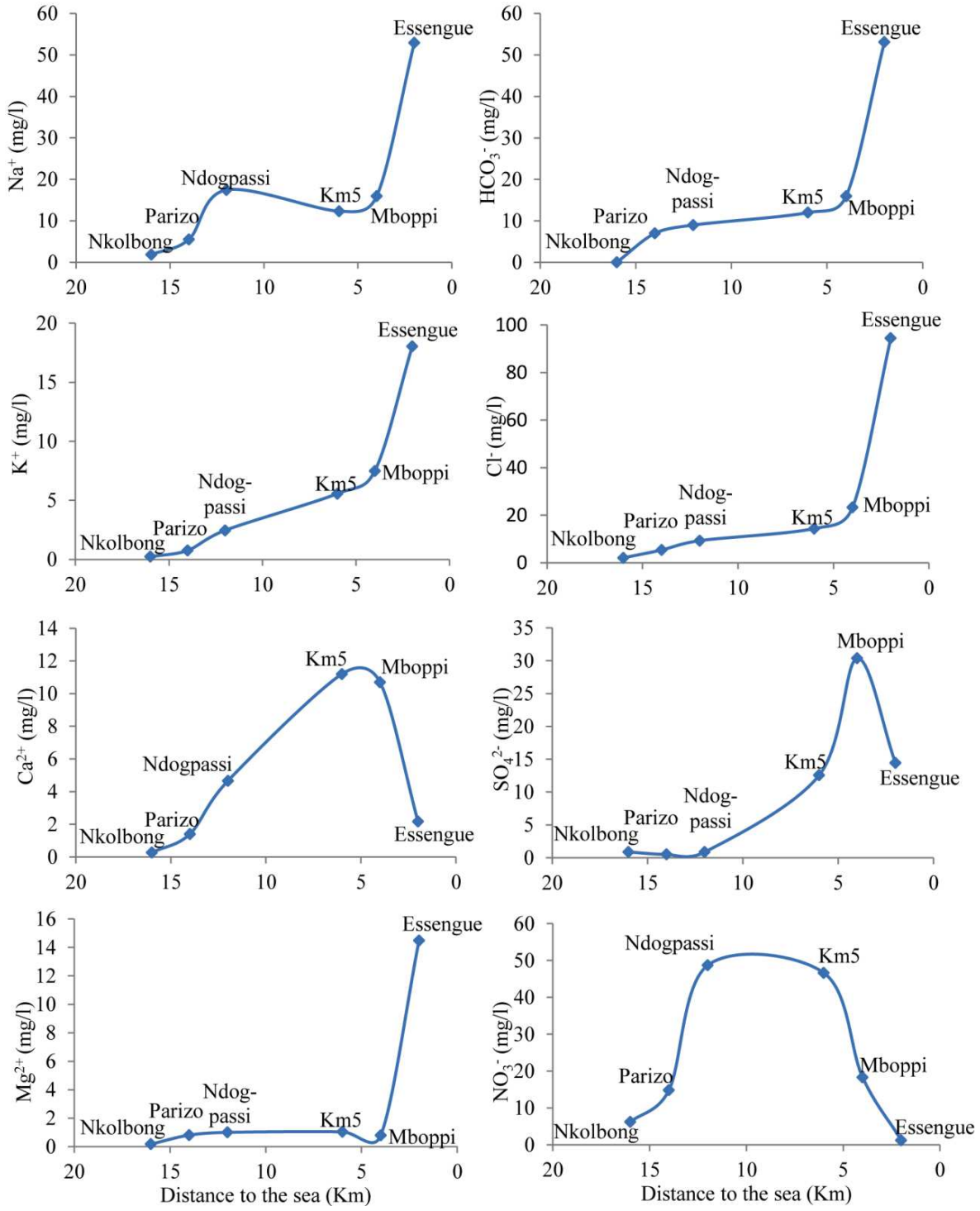

Fig. 10 Evolution of major ions concentrations along the groundwater flow path from Nkolbong (upstream, SE side of the Douala region), to Essengue (downstream, NW side of the Douala region) according to the E-F transect shown in Fig. 6.

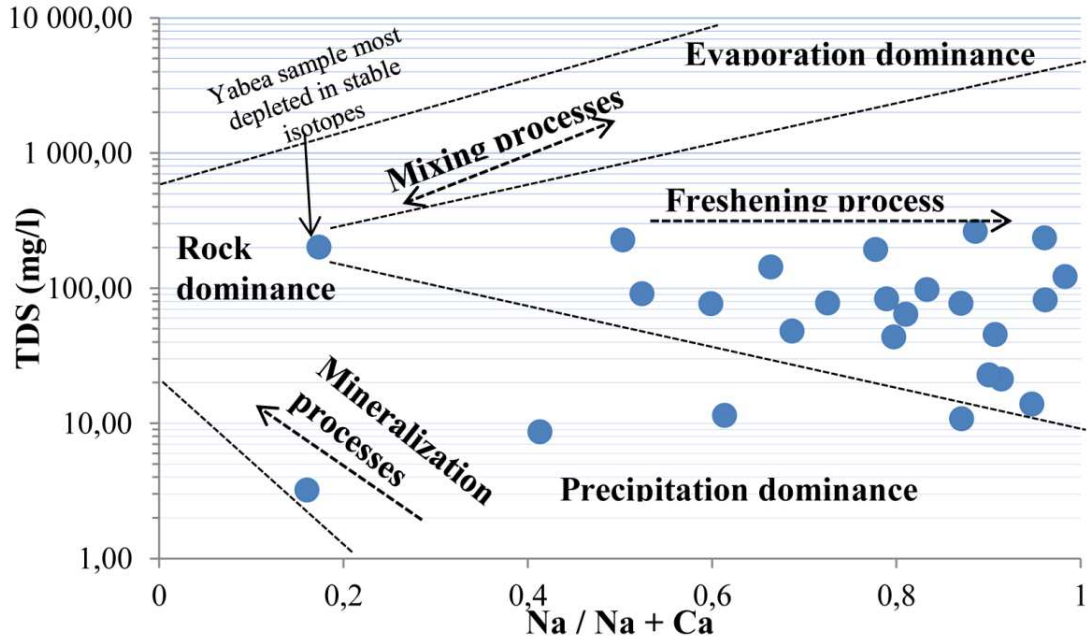

Fig. 11 Gibbs diagram for deep Mio-Pliocene groundwater at Douala.

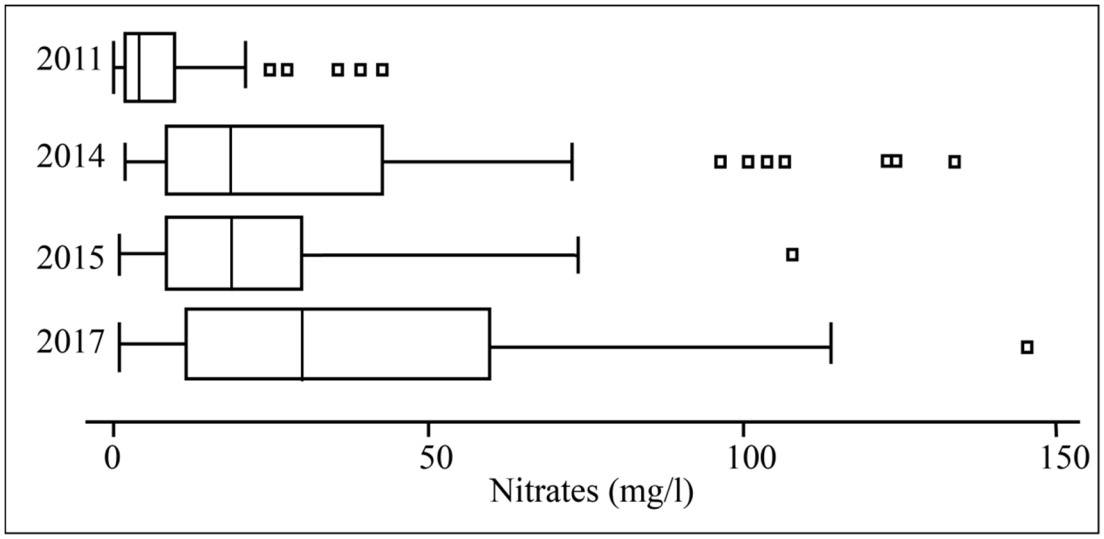

Fig. 12 Box whisker plot illustrating the temporal evolution of NO_3^- over the years on the Mio-Pliocene aquifer at Douala, Cameroon.

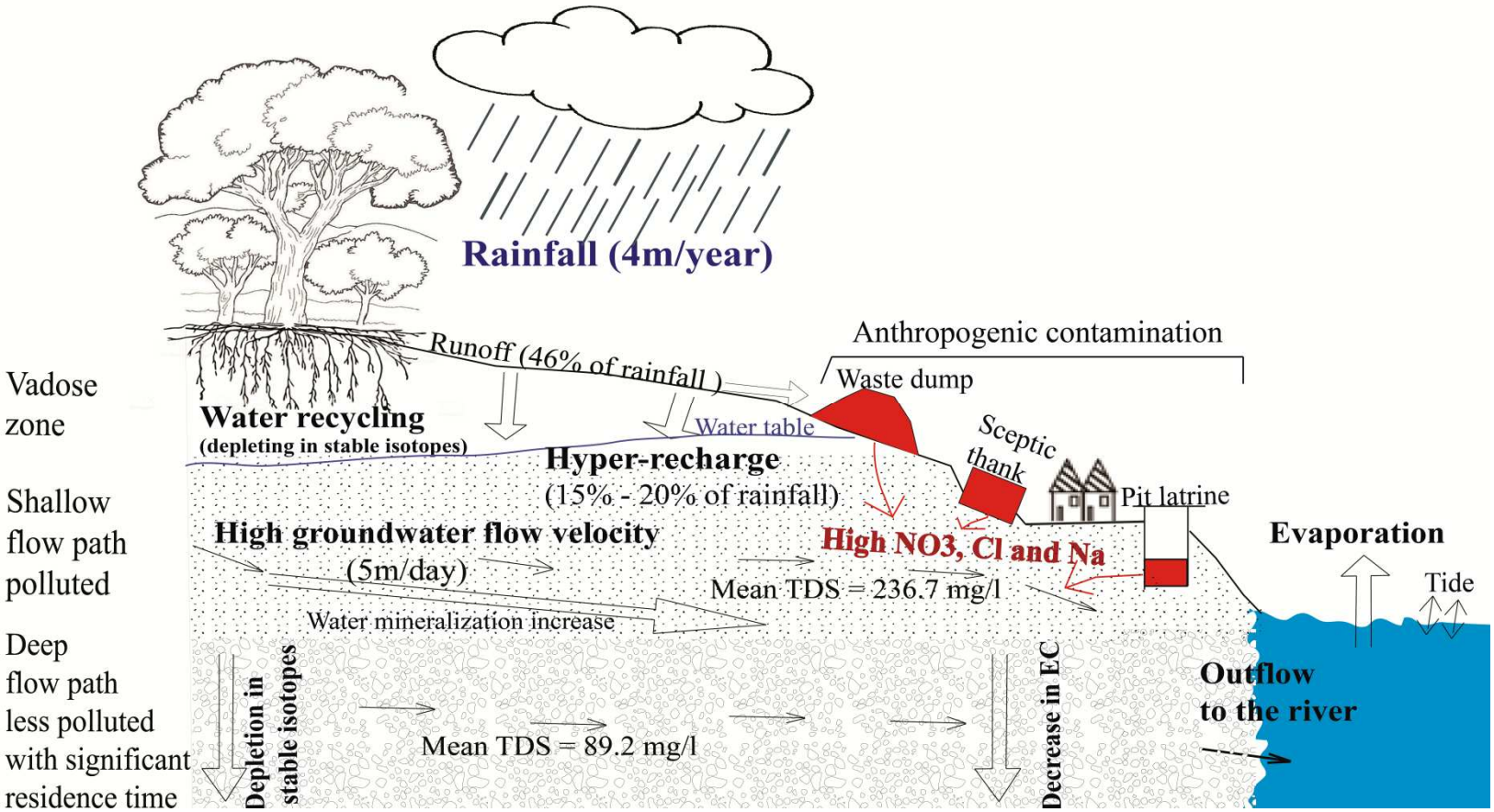

Fig. 13 Synthesis of hydrological functioning of Mio-Pliocene aquifer at Douala

List of Tables

Table 1 Hydro-stratigraphy of the Mio-Pliocene aquifer.

Age	**Lithology**	**Thickness**	**Hydrogeological characteristic**
Pliocene	Clay, sandy-clay, clayey-sands	0 - 40 m	Aquiclude/aquitard/aquifer
Lower Miocene	Cross-bedded sands with passages of lignite and limestone	>220 m	Aquifer
Upper Miocene	Coarse grained sand (slightly silty and calcareous) Gravel		

Table 2 Hydrodynamics settings of the Mio-Pliocene aquifer in Douala. Data were collected from historical records of drillings (n= 68) for water wells.

	Mean	**Minimum**	**Maximum**	**Standard deviation**
Transmissivity (m^2/s)	5.6×10^{-3}	4.6×10^{-4}	6.8×10^{-2}	6.1×10^{-3}
Hydraulic conductivity (m/s)	1.5×10^{-3}	2.6×10^{-5} m/s	0.2 m/s	0.03

Table 3 Descriptive statistics of chemical parameters. Concentrations of major ions are expressed in mg/L.

		Groundwater from boreholes (n = 26)					**Groundwater from hand-dug wells (n = 18)**					**Groundwater from springs (n = 10)**				
Parameter	Unit	Min	Max	Mean	Med	SD	Min	Max	Mean	Med	SD	Min	Max	Mean	Med	SD
pH		3	8.5	4.7	4.4	0.9	3.2	7.6	5.7	5.8	0.8	3.3	7.6	4.9	4.8	1.1
Temp.	°C	27.4	31.5	28.9	28.6	1	27.8	29	28.3	28.2	0.4	27.2	29.8	28	27.9	0.7
EC	µS/m	13.6	1632	200.7	105.8	318.9	47	1048	428.4	399.5	268.8	111.8	375	255.3	274	85
DO	mg/l	2.3	7.8	6	6.5	1.4	2.2	7	4.5	4.4	1.4	2	7.8	4.3	4.3	1.8
K^+	mg/l	0.1	19.3	4.7	2.9	5.4	1	41	12.4	10.6	10.3	2.3	11.7	6.8	6.7	3.6
Na^+	mg/l	0.0	52.9	15.8	13.1	14.5	4.7	86.9	36.6	37.6	23.5	9.7	60.8	28	24.7	13.7
Ca^{2+}	mg/l	0.2	32.9	5.4	3	7.4	1.8	81.1	24.7	22.9	21.4	1.4	21.3	7.7	6	6.4
Mg^{2+}	mg/l	0.1	21.4	2.3	0.8	4.8	0.3	6.7	2	1.3	1.7	0.5	1.7	1	0.9	0.3
Cl^-	mg/l	1.6	94.4	17.1	7.4	20.9	4.3	131.1	50.4	45.9	38.8	6.8	72.1	40	30	19.4
SO_4^{2-}	mg/l	0.5	44.7	7.2	1.6	11.9	0.8	90.5	35	43.8	26	0.7	33.4	9.3	4.9	10.3
HCO_3^-	mg/l	0	137	9.4	0	28.8	0	222.2	28.9	0.4	68.9	0	0	0	0	0
NO_3^-	mg/l	1.1	145.5	35	26.1	36.1	7.6	245.6	56.7	43.6	56.1	28.2	93.4	61.6	61	21.6

Table 4 Estimated NBLs* and TV** of parameters for the MP aquifer at Douala. Reference (Ref) used are those defined by WHO (2011).

Parameters	Ref	NBLs		TV	Number of samples above the NBL (%)			Number of samples above the TV (%)		
		Min	Max		Boreholes	Hand-dug wells	Springs	Boreholes	Hand-dug wells	Springs
EC (µS/cm)	250	13.6	41.3	145.7	73.1	100	100	38.5	77.8	90
K^+ (mg/l)	100	0.1	0.5	50.3	76.9	100	100	0	0	0
Na^+ (mg/l)	200	0.04	6.7	103.4	65.4	88.9	100	0	0	0
Ca^{2+} (mg/l)	75	0.2	1.1	38.1	65.4	100	100	0	15.4	0
Mg^{2+} (mg/l)	30	0.1	0.8	15.4	61.5	83.3	80	0	0	0
Cl^- (mg/l)	250	1.6	4	127	69.2	100	100	0	5.6	0
SO_4^{2-} (mg/l)	250	0.5	1.5	125.8	30.8	88.9	80	0	0	0
HCO_3^- (mg/l)	200	0	9	104.5	15.4	11	0	3.9	5.6	0
NO_3^- (mg/l)	50	1.1	6.6	28.3	26.9	100	100	46.1	66.7	100

*NBLs = Natural background levels, **TV = Threshold values

Shallow urban aquifers under hyper-recharge equatorial conditions and strong anthropogenic constrains. Implications in terms of groundwater resources potential and integrated water resources management strategies.

Graphical abstract